

# Chapter 1

## 1.1 Introduction

### 1.1.1 General introduction to foot-and-mouth disease

The recent outbreaks of foot-and-mouth disease (FMD) in a number of FMD-free countries, in particular Taiwan in 1997 and the United Kingdom in 2001, have significantly increased public awareness of this highly infectious disease of cloven-hoofed livestock. Outbreaks have occurred in every livestock-containing region of the world with the exception of New Zealand, and the disease is currently enzootic in all continents except Australia and North America (**Figure 1.1**). The disease affects domestic cloven-hoofed animals, including cattle, swine, sheep, and goats, as well as more than 70 species of wild animals, including deer, and is characterized by fever, lameness, and vesicular lesions on the tongue, feet, snout, and teats [1]. Although FMD does not result in high mortality in adult animals, the disease has debilitating effects, including weight loss, decrease in milk production, and loss of draught power, resulting in a loss in productivity for a considerable time. Mortality, however, can be high in young animals, where the virus can affect the heart. In addition, cattle, sheep, and goats can become carriers, and cattle can harbor virus for up to 2 to 3 years [2].

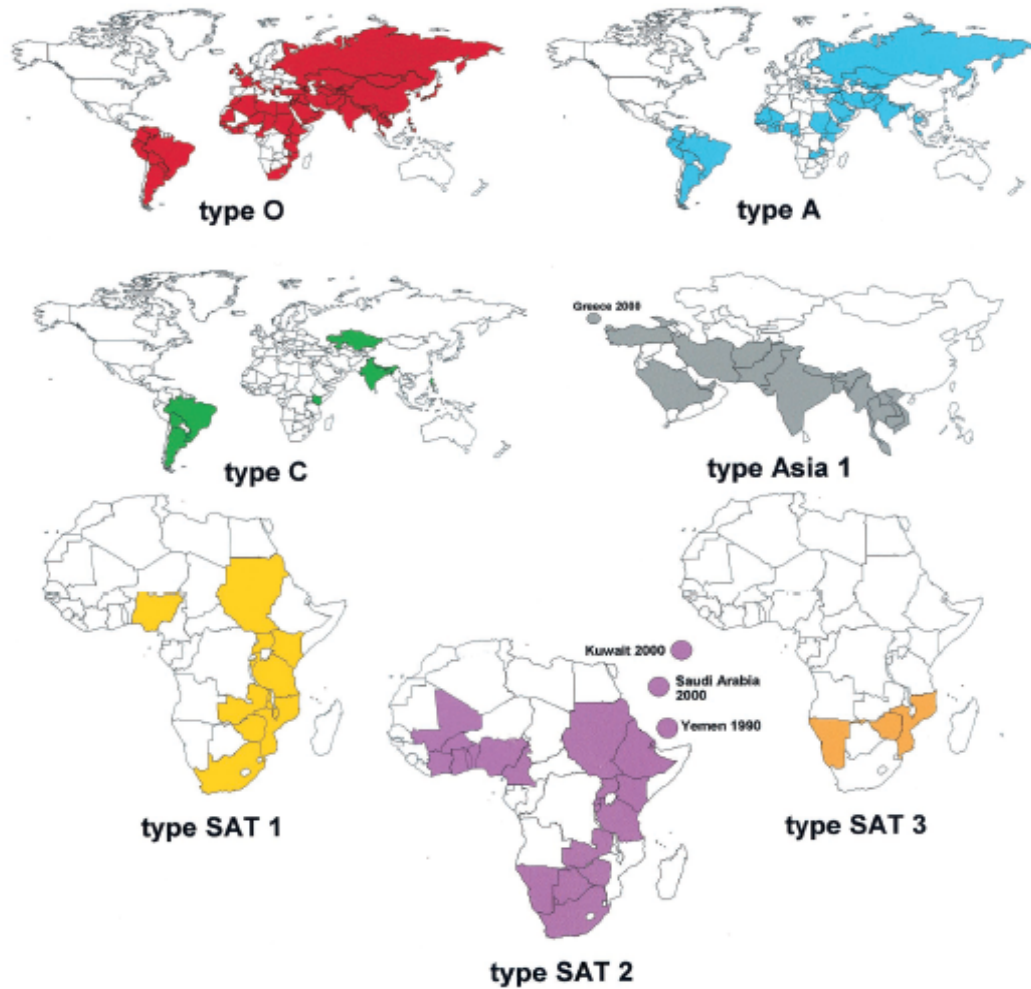


FIG. 1. Countries in which FMD was reported to the OIE between 1990 and 2002. The data and maps were compiled by Nick Knowles

**Figure 1.1** Countries in which FMDV was reported to the OIE between 1990 and 2002 [1]

### 1.1.2. The outbreak of foot-and-mouth disease in Taiwan

The foot-and-mouth disease had originated in India in 1990 and spread through the Middle East, Turkey, and Eastern Europe. It then moved eastward into the People’s Republic of China in 1999 and then to Taiwan, South Korea, Japan, Mongolia, and far-east Russia. The virus then appeared in South Africa in late 2000 and in the United Kingdom in February 2001 (**Figure 1.2**).

The outbreak in Taiwan, caused by a type O virus /Taiwan/97, was first reported in

March 1997 and within 3 weeks spread to almost the entire island, demonstrating the ability of the virus to replicate and spread at an alarming rate [3, 4]. Taiwan was declared an FMD-infected zone and lost its pork export market. The outbreak was controlled by a combination of slaughter of infected animals and vaccination. An interesting observation during this outbreak was that disease was found only in pigs and did not occur in cattle or goats that were also present on some of the infected farms [3, 4].

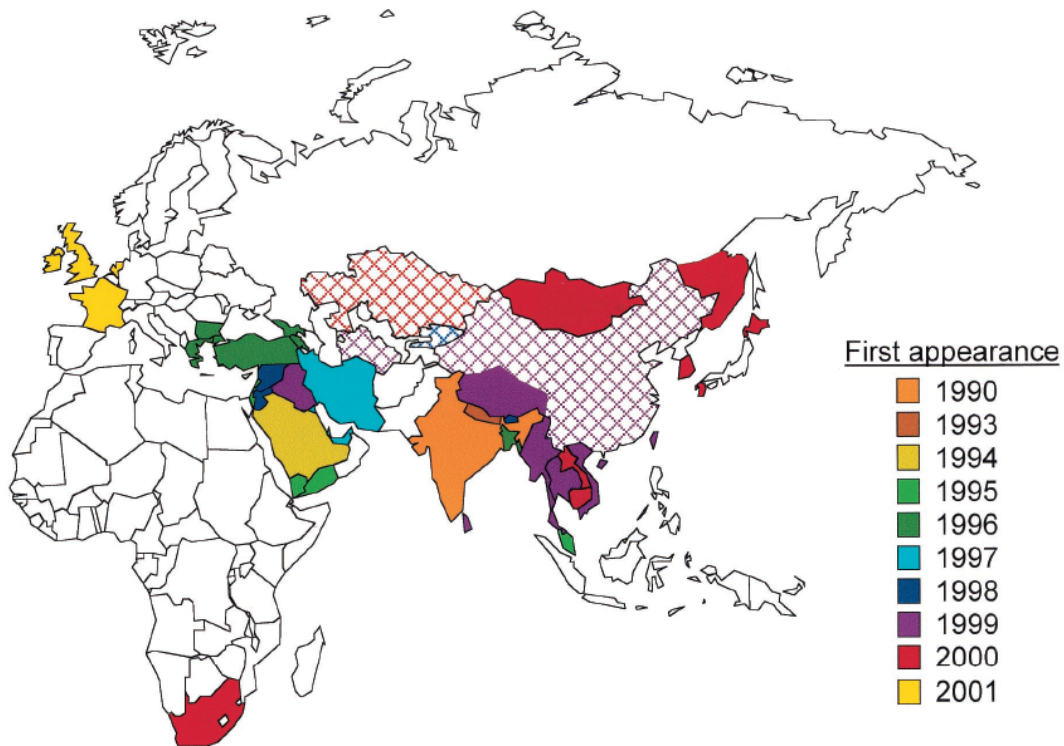


**Figure 1.2** The spread of the PanAsian strain of FMDV type O from its first appearance in India in 1990 until its appearance in the United Kingdom in 2001. Solid colors, PanAsian strain present; cross-hatched colors, type O present and PanAsian strain suspected [1].

### 1.1.3. The structure of foot-and-mouth disease virus

Foot-and-mouth disease virus (FMDV) is a small, non-enveloped, icosahedra virus with a single-stranded RNA genome of approximately 8400 nucleotides. By electron microscopy, the FMDV appears to be a round particle with a smooth surface and a diameter of about 25 nm [5]. The fine structure of the viral capsid has been determined for a number of serotypes by using X-ray crystallographic techniques [6], and the structural features of type O are shown (**Figure 1.3A**). An unusual structural feature of the outer capsid surface is a long and flexible loop of the VP1 protein [7, 8] (**Figure 1.3B**). This loop, namely G–H loop, forms a major antigenic site on the virus and includes at its apex an Arg-Gly-Asp (RGD) motif [9, 10]. Amino acids in this loop contain both immunodominant T and B epitopes that can elicit neutralizing antibody response; so many studies try to use G–H loop to be peptide vaccine.

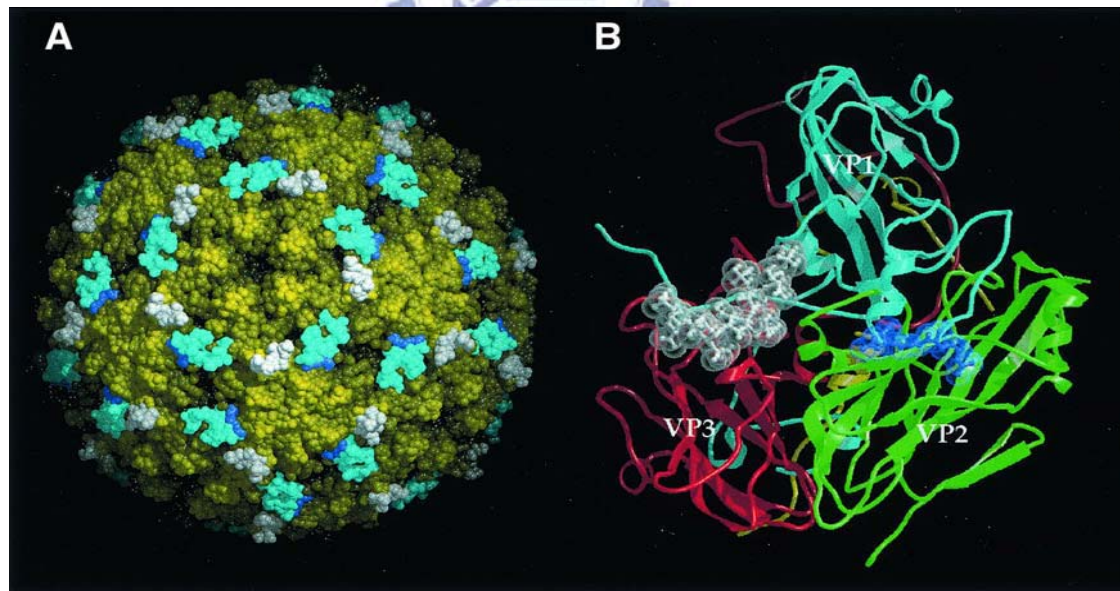
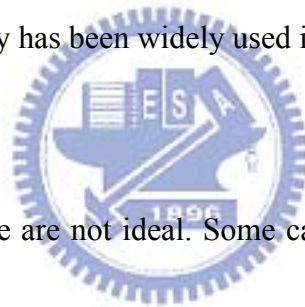


**Figure 1.3** (A) Structure of the mature type O FMDV virus based on X-ray crystallographic data (B) The organization of the entire virion, highlighting the G-H loop (yellow) and the RGD sequence (purple). All structures are representative of the mature virion, and the viral

proteins are colored blue (VP1), green (VP2), and red (VP3) [6].

#### **1.1.4. Peptide Vaccine**

Synthetic peptides have been applied as vaccines in recent years; however carriers are needed for efficient immune response. Peptides are generally not immunogenic enough to elicit high levels of antibody response. To enhance the immune response, peptides are coupled to carrier molecules to form peptide-carrier constructs. Large proteins or toxoids are regularly used as carriers, such as keyhole limpet hemocyanin (KLH) [11, 12], ovalbumin (OVA) [13, 14], bovine serum albumin (BSA) [15, 16], and tetanus toxoid (TT) [17, 18]. Moreover, this kind of peptide vaccine technology has been widely used in influenza [19, 20] or other disease [8] vaccines recently.



Most carriers currently in use are not ideal. Some carrier proteins elicit strong antibody responses and suppress immune-response of peptide. For biological compounds, only few conjugation sites are available, leading to insufficient presentation of epitope and most important of all also exposing unnecessary antigenic sites of carriers themselves. Many carrier proteins are not stable in solution and conjugation between carrier protein and peptide often results in precipitates, causing non-reproducible conjugation and complicated analysis of end products. The major drawbacks indicate the need for improved carrier molecules.

#### **1.1.5. The advantage of gold nanoparticle served as vaccine carrier**

To serve as a general carrier, basic parameters such as the toxicity, immunogenicity, and specificity need to be characterized. Gold nanoparticles (GNPs) have been previously applied as immunogenic carriers such as drug delivery [21], cancer cell imaging [22], and photo-activated therapeutic [23], and as antigen carrier for the antibody generation [24-27].

GNPs possess many advantages as vaccine carrier. Synthesis of GNPs has been studied for decades and the reaction is well known and the wet chemistry is easy to operate in laboratory. GNP is synthesized as a specific size which is controlled by the reaction conditions. GNPs are stable in solution. The aggregation of GNPs causes color change and can be traced visually. Gold is one of the best biocompatible materials. Gold has unusual affinity to sulfhydryl group, thus tight conjugation to peptide is achieved by the addition of extra cysteine residue to the peptide. However, as a general vaccine carrier, the in vivo toxicity, immunogenicity, and specificity, and most important of all, the size dependency of GNPs is not clear at the present time.

### **1.1.6. Motivation**

The purpose of this study is to investigate the potential role of gold nanoparticles as vaccine carrier. Immunogenicity and specificity was evaluated using KLH as control. Particularly, size has been played a pivotal role in the endocytosis and toxicity of GNPs to cells [28-30] and animals [31-33]. It is foreseeable that size may play an important role for

GNPs as a vaccine carrier.



## 1.2. Materials and Methods

### 1.2.1. Chemicals

HAuCl<sub>4</sub>, sodium citrate, NaBH<sub>4</sub>, HCl, HNO<sub>3</sub>, H<sub>2</sub>SO<sub>4</sub>, H<sub>2</sub>O<sub>2</sub>, and other chemicals of analytical grade were purchased from Sigma-Aldrich and Fisher. H<sub>2</sub>O was >18 MΩ from a Milli-Q water purification system.

### 1.2.2. Preparation and characterization of gold nanoparticle

Gold nanoparticles (GNPs) of diameter with 2 nm, 5 nm, 8 nm, 12 nm, 17 nm, 37 nm, and 50 nm were synthesized as reported previously [34, 35]. The seed colloids were prepared by adding 1 mL of 0.25 mM HAuCl<sub>4</sub> to 90 mL of H<sub>2</sub>O and stirred for 1 min at 25 °C. Two milliliters of 38.8 mM sodium citrate were added to the solution and stirred for 1 min, followed by the addition of 0.6 mL of freshly prepared 0.1 M NaBH<sub>4</sub> in 38.8 mM sodium citrate. Different diameters of GNPs ranging from 2 nm to 50 nm were generated by changing the volume of seed colloid added. The solution was stirred for an additional 5-10 min at 0-4 °C. Reaction temperatures and times were adjusted to obtain GNPs of larger size. All synthesized GNPS were characterized by UV absorbance. The size of synthesized GNPs was verified by electron microscopy and atomic force microscopy. GNPs were dialyzed against phosphate-buffered saline (pH 7.4) before injection into the animals.



### 1.2.3. Designing of Synthetic peptide

The sequence of FMDV peptide (pFMDV) is NGSSKYGDTSTNNVRGDL QVLAQKAERTL(C), representing the amino acid residues 131–159 of VP1 of the FMDV O/Taiwan/97strain, was synthesized with COOH-terminal cysteine residues using an ABI peptide synthesizer and Fmoc chemistry. Its amino acid sequence was verified by mass spectrometry and amino acid composition analysis.

### 1.2.4. Preparation of pFMDV-carrier conjugates

For preparing KLH conjugates, were synthesized as reported previously [8] , pFMDV containing cysteine was resuspended in Milli-Q water at 1 mg/ml, and the pH was adjusted to approximately 8.5 by addition of dilute NaOH. Commercial maleimide-activated KLH (Pierce. ALEX, IL) was reconstitute in 50mM sodium phosphate, 0.15M NaCl, 0.1M EDTA, pH 7.2 buffer at 10 mg/ml. Peptide and carrier were mixed at a 0.5 molar ratio of thiol to maleimide in 0.1M sodium phosphate, 0.15M NaCl, 10mM EDTA, pH 7.2 buffer and allowed to react in the dark at 25 °C. The conjugated complexes were purified by centrifugation and resuspended in PBS to final concentration (0.01 ug/ul). The conjugate was separated from unreacted peptide and carrier by HPLC.

For preparing Gold nanoparticle conjugates, the approach used to conjugate the gold nanoparticles with peptide was based on titration methods [36]. An extra cysteine was added

to the C-terminus of each peptide in order to improve binding to the gold surface. Conjugation of antigen with GNPs was performed by titration the antigens into a GNP solution. The titration was monitored by UV absorption at the wavelength appropriate for each peptide to detect aggregation of unsaturated GNP in the presence of 1 M sodium chloride. After reaching the saturation point, the conjugated complexes were purified by centrifugation and resuspended in PBS to final concentration (0.01 ug/ul)

### **1.2.5. Immunization of mice**

Animal treatments were performed following “The Guidelines for the Care and Use of Experimental Animals” of National Chiao Tung University. Four-week-old male BALB/C mice were housed at  $22\pm 2$  °C with a 12-h light/dark cycle and fed standard rodent chow and water ad libitum. Mice were randomly assigned to experimental groups. Each group consisted of 6 mice.

Groups of 4-week-old BALB/c mice were given intraperitoneal (IP) and subcutaneous (SC) immunizations with: (1) pFMDV-KLH conjugate and (2) pFMDV-GNPs conjugates with sizes of 2-nm, 5-nm, 8 nm, 12-nm, 17-nm, 37-nm and 50-nm. Those antigens were administered with equal volume of complete and incomplete adjuvant.

For all groups, the mice were immunized on week 0, 1, 2, 3, 5, 7 and 9, and the blood was collected from tail vein after week 4, 6, 8, and 10. The sera were collected after

centrifugation and stored at  $-20^{\circ}\text{C}$ . Animals were sacrificed at the end of experiment by cardiac puncture under  $\text{CO}_2$  anaesthesia. The spleens were isolated and organ weights of all mice were measured.

### **1.2.6 Enzyme-linked immunosorbent assay (ELISA)**

In order to coat wells with GNP as an antigen, each microwell of a 96-well Corning plate was pre-treated with 200  $\mu\text{L}$  of 1 mM 3-aminopropyl-triethoxysilane (APTES) in ethanol at room temperature for 40 min. The activated wells were washed with ethanol twice for 5 min, followed by distilled water for 5 min. Gold nanoparticles (15mM, 150uL) were added to the microwells and incubated for 2 h at room temperature, followed by three Milli-Q water washes and finally with three washes with 0.5% Triton X-100 in PBS. To coat wells with other antigens, 100  $\mu\text{L}$  of antigen was added into microwells and incubated at room temperature for 30 min, followed by three PBS washes. Blocking for non-specific binding was performed by adding 100  $\mu\text{L}$  of 3% BSA and incubating for 60 min at room temperature, followed by three PBS washes. Binding was performed by adding 100  $\mu\text{L}$  of diluted antiserum into microwells and incubating for 1 hr at room temperature, followed by thorough washes. HRP-conjugate danti-mouse IgG, 2,2'-azino-di-(3 ethylbenzthiazoline sulfonic acid) (ABTS) and  $\text{H}_2\text{O}_2$  were added in sequence to the wells according to the manufacturer's protocol, and the binding efficiency was monitored by measuring absorbance at 405 nm.

### **1.2.7. Gel-Electrophoresis of GNPs**

Samples were mixed with 1% TBS (Sigma) and loaded onto 3% agarose gel (Sigma). Gel separation was performed using the electrophoresis unit running at 80 V. Protein levels were visualized by incubating the gels in Coomassie Brilliant Blue R-250 staining solution (Sigma). Gels were washed with a destaining solution containing 70% methanol and 7% acetic acid.

### **1.2.8 Inductively coupled plasma mass spectrometry (ICP-MS)**

For the total elements determinations, standard solutions were prepared by dilution of a multi-element standard (1,000 mg L<sup>-1</sup> in 1 M HNO<sub>3</sub>) obtained from Merck (Darmstadt, Germany). Nitric acid (65%), hydrochloric acid (37%), perchloric acid (70%), and hydrogen peroxide (30%) of Suprapur® grade (Merck) were used to mineralize the samples. A size-exclusion column was connected to the ICP-MS apparatus. Spleen section samples were homogenized in 25 mM tris (hydroxymethyl) aminomethane (Tris)–12.5 mM HCl buffer solution at pH 8 and centrifuged at 13,000 rpm for 1 h. The supernatant was applied to the size-exclusion column of the HPLC system, which had been equilibrated with 25 mM Tris–12.5 mM HCl (containing 20 mM KCl), and eluted with the same buffer at a flow rate of 1 mL/min. The metal components of metal-binding proteins that were eluted from the HPLC system were detected by ICP-MS (Perkin Elmer, SCIEX ELAN 5000). The main instrumental

operating conditions were as follows: RF power 1900 W, carrier gas flow 0.8 L/min Ar and makeup gas flow 0.19 L/min Ar. The following isotopes were measured:  $^{197}\text{Au}$  as internal standard.

### **1.2.9 Transmission electron microscopy (TEM)**

Small pieces of unfixed tissue were fixed in 2.5% glutaraldehyde with 0.05 M sodium cacodylate-buffered saline (pH 7.4) at room temperature for 2 h. The primary fixation was followed by three 0.05 M sodium cacodylate-buffered saline washes (pH 7.4) for 20 min each. The samples were then placed into a 1%  $\text{OsO}_4$  in the same buffer at room temperature for 1 h.  $\text{OsO}_4$  fixation was followed by three 20 min distilled-water washes and dehydration in acetone. The samples were transferred successively to 33% and 66% Spurr resin/acetone solutions. The samples were left for 30 min in each solution. The samples were then transferred to 100% Spurr resin first for 5 h and then in fresh resin overnight. Ultrathin sections were made using an ultra microtome and sectioning the samples into 100-nm sections. The grids with ultrathin sections were post-stained with uranyl acetate for 30 min followed by lead for 3 min. After the post-staining procedure, a thin layer of carbon was evaporated onto the surfaces of the grids. Ultrathin-sectioned material was examined with a Jeol 1400 and a 3200 FS TEM.

### **1.2.10. Statistical Analyses**

All data are presented as means  $\pm$  S.E.M. with a minimum of six mice in each group.

Concentrations of biogenic amines and Ach in spleen were analyzed using the unpaired student *t*-test. The criterion for statistical significance was  $p < 0.05$  for all statistical evaluations.



## 1.3: Result and Discussion

### 1.3.1. Preparation and analysis of pFMDV-GNP conjugates

To further investigate the utility of GNPs as vaccine carrier, pFMDV was designed and synthesized based on the immunogenic epitope previously reported. In particular, an extra cysteine residue was attached to the C-terminus of the peptide to provide sulfhydryl group as conjugating site with GNPs. The pFMDV was conjugated to GNPs of various sizes (2-nm, 5-nm, 8-nm, 12-nm, 17-nm, 37-nm and 50-nm).

Synthesis of GNPs with varied sizes was monitored by UV absorbance (**Figure 1.4**) and examined by electron microscopy (**Figure 1.5**). Conjugation of pFMDV-GNP was optimized by NaCl-induced aggregation [36]. The lowest concentration of peptide that did not cause a color change from red to dark blue was chosen for conjugation. The amount of pFMDV conjugated per GNP was also calculated (**Figure 1.6**) which is proportional to the surface areas of GNPs. Conjugation of peptide to GNPs was analyzed by electrophoresis (**Figure 1.7**). Tight and focuses bands of pFMDV -GNPs indicated stable conjugates were generated.

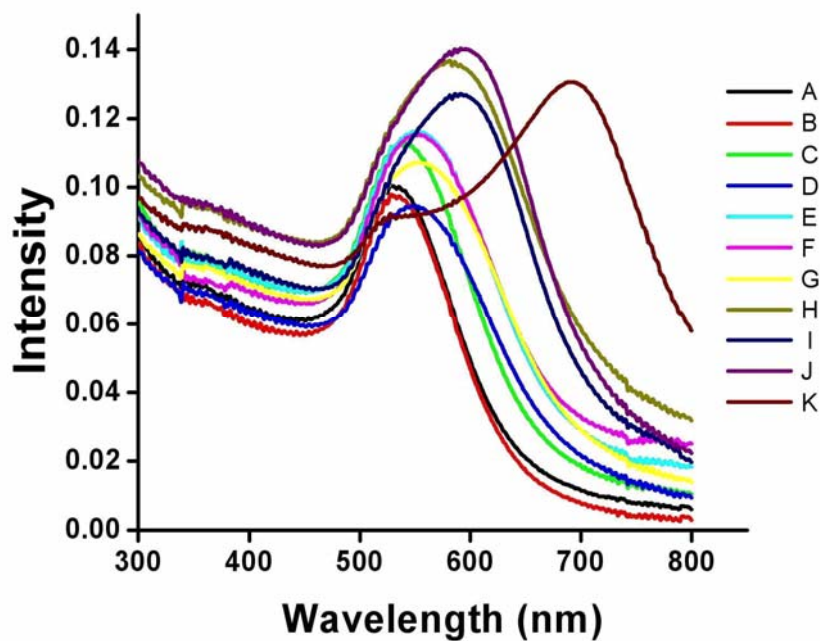


**Figure 1.4** UV-Vis absorbance measurements of GNPs with shift of the surface plasmon band peaks correlating with peptide of different concentrations.

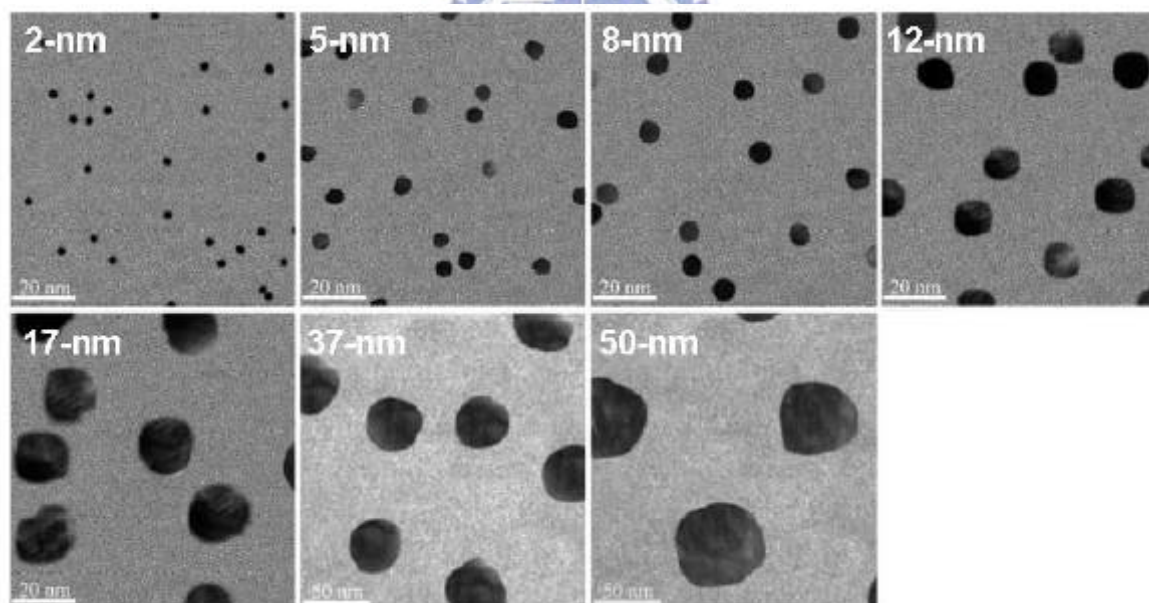


**Figure 1.5** TEM images for the GNPs synthesized in the current study. GNPs with diameters of 2-nm, 5-nm, 8-nm, 12-nm, 17-nm, 37-nm, and 50-nm were examined under an electron microscope. Scale bars are 20-nm for images of 2-nm, 5-nm, 8-nm, 12-nm, and 17-nm GNPs. Scale bars are 50-nm for images of 37-nm, and 50-nm GNPs.



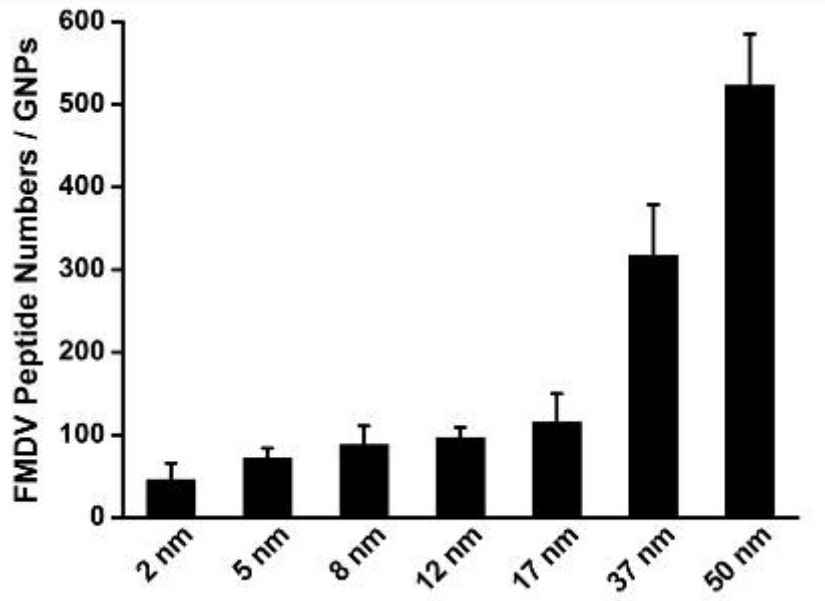


**Figure 1.6** Number of pFMDV conjugated to GNP versus the diameter of GNP. The amount of conjugated FMDV peptide on GNPs surface is calculated from the saturation concentration of the titration curves. The amount of conjugated pFMDV is proportional to the surface area of GNPs.

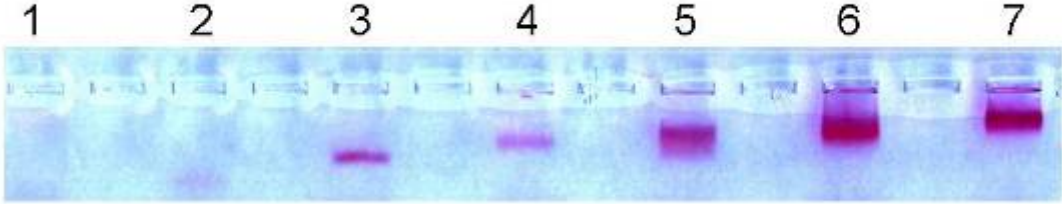


**Figure 1.7** Gel electrophoresis of pFMDV-GNP conjugates. Electrophoresis is performed without staining. The difference in the mobility of protein bands was attributed to the differences in the size of GNPs adsorbed to FMDV peptide. pFMDV-GNP conjugates loaded on each lane: lane 1, 2-nm GNP; lane 2, 5-nm GNP; lane 3, 8-nm GNP; lane 4, 12-nm GNP; lane 5, 17-nm GNP; lane 6, 37-nm GNP; and lane 7, 50-nm GNP.

It is possible the immune response of pFMDV is proportional to number of peptide absorbed on GNPs. However, the total amount of peptide in each injection is constant. Furthermore, as elicited by titration test and gel electrophoresis, the number of peptide per GNP is proportional to the surface area of GNP but not correlated with the size-dependent immune response profile.

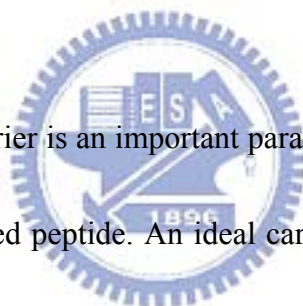
### **1.3.2 The pFMDV-GNP conjugates induced focused and enhanced antibody response**

Mice were immunized with pFMDV-GNP conjugates with varied sizes of GNPs. Each injection contains equal amount of pFMDV-GNP conjugates (0.01  $\mu$ g/ul). For control experiment, mice were injected with pFMDV-KLH conjugates (0.01  $\mu$ g/ul). These conjugates were injected intraperitoneally and subcutaneously into BALB/C mice weekly from week 0. Tail blood was withdrawn at week 4, 6, 8, and 10. ELISA was performed to obtain titers of antisera against pFMDV, GNPs, and KLH (**Figure1.8 and Figure1.9**).

Significant antibody response appeared for antisera withdrawn on week 6 (**Figure1.8**). The binding affinity using pFMDV as antigen showed a size-dependent profile. The pFMDV-2-nm GNP induced titer of 18,000 $\pm$ 300 at week 6. The induced titers increased when the size of GNPs increased, maximized at 8 nm of 61,000 $\pm$ 2700, and decreased to 0 for 37 nm and 50 nm. The pFMDV-KLH conjugate exhibited medium antibody response with titer of

20,000. A 3.4-fold enhancement of antibody response was observed compared to the use of KLH as carrier.

When antibody responses of week 4, 6, 8, and 10 were integrated, a clearly size-dependent tendency was observed (**Figure 1.9A**). GNPs (ranging from 2-nm to 8-nm) exhibited increasing binding affinity following subsequent immunizations. Highest binding activity was associated with 8-nm GNP. Gradual decrease in titer was observed for 12-nm and 17-nm GNPs. We could not observe induced binding activity for 37-nm and 50-nm GNP conjugates until the end of experiment. KLH conjugate remained medium binding affinity compared to GNP conjugates.



Antibody response to the carrier is an important parameter which determines the focused immunogenicity of the conjugated peptide. An ideal carrier should remain silent during the immunization of peptide conjugates. KLH and other carriers are known to induce significant immune response [37, 38, 12]. The binding activity of antiserum against KLH was observed from week 4 and increased to a significant level of 11,000 on week 10 (**Figure 1.9B**). On the contrary, GNPs regardless of the size showed no detectable binding activity during the course of our experiment. GNPs are demonstrated to be ideal candidates as vaccine carrier for their insensitivity to immune system.

Here we show GNPs as vaccine carriers, compared to KLH, exhibited approximately 3.4-fold enhancement of immunogenicity and apparently no detectable binding activity to themselves. Thus GNPs displayed all characteristics for an ideal vaccine carrier.

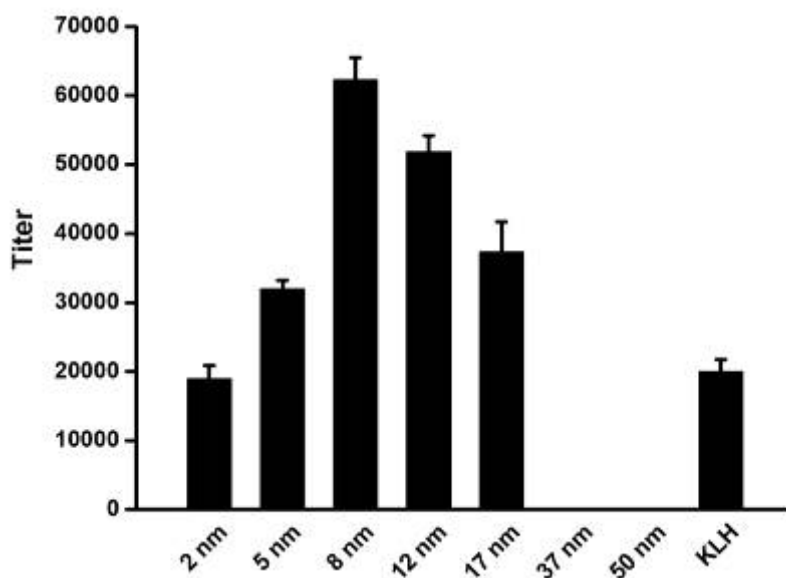


**Figure 1.8** Titers of antiserum withdrawn from pFMDV-GNPs injected mice on fourth week of immunizations against pFMDV. The values are averaged from 6 independent mice. Titer of pFMDV-KLH serves as control. Sera obtained from pFMDV-37-nm GNP and pFMDV-50-nm GNP injected mice do not show detectable binding activity.

It was reported that KLH conjugate exhibits strong immune response. KLH also exhibits non-specifically binding to the antigen and give rise to false positive binding of cross reactivity. KLH as a carrier exhibited high immune response against itself with the titer even higher than anti-pFMDV (**Figure 1.9**). It is likely that conjugation of pFMDV with KLH generated potent recognition sites, thus complicated the induced antibody species. The

antibodies strongly recognize pFMDV-KLH conjugates and KLH. Specific binding against the synthetic FMDV peptide would be seriously reduced.

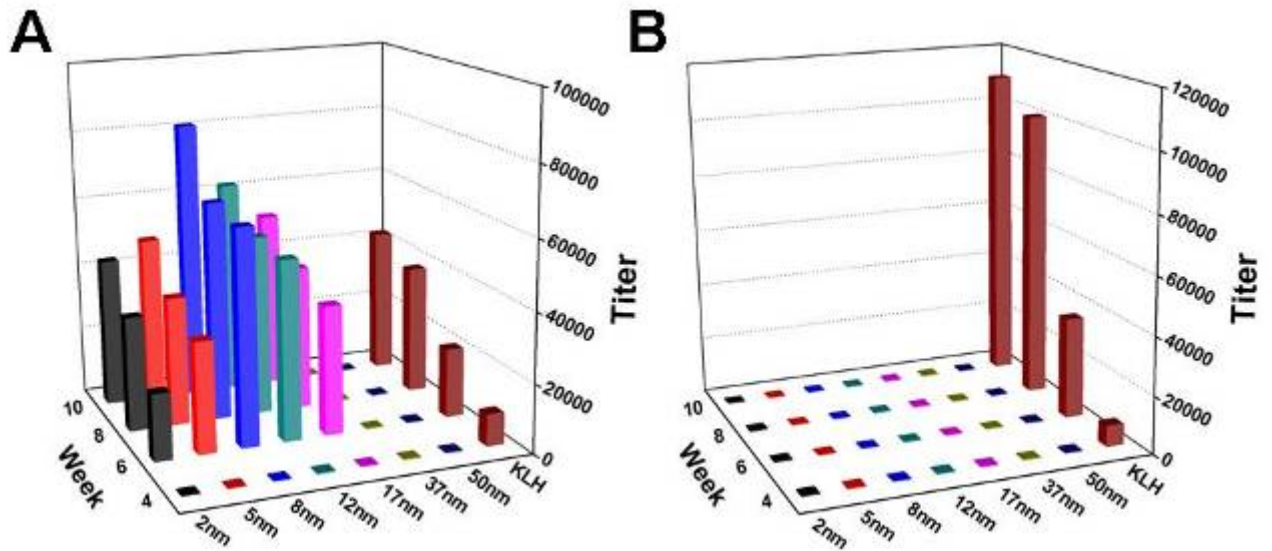


**Figure 1.9** Titers of antisera withdrawn from pFMDV-GNPs injected mice on week 4, 6, 8 and 10. The antigens used in the ELISA are (A) pFMDV (B) GNP/KLH. Titers of pFMDV-KLH are incorporated as control.

Compared to KLH carrier, GNPs as a carrier exhibit undetectable antibody response. However, when conjugated with pFMDV-GNP showed strong antibody response against pFMDV. It indicated that antibody response against synthetic pFMDV was not altered by the conjugation of carrier.

The result indicated that antibody response to pFMDV-GNPs selectively resided and focused on the conjugated peptide (**Figure 1.10**), while antibodies responding to

pFMDV-KLH treated KLH as additional immune targets. GNPs are demonstrated to be ideal candidates as vaccine carrier for their inert to immune system.

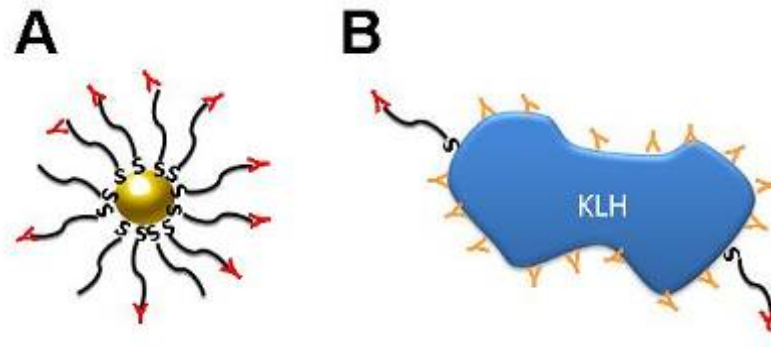


**Figure 1.10** (A) The antibody focused recognizes the pFMDV adsorbed on surface of GNPs

(B) The antibody recognizes both pFMDV and KLH so that reduce the binding activity of pH5N1.



In rare events, naked GNPs might induce antibody response which might affect the immunogenicity and specificity of pFMDV-GNP conjugates. In previous study [39], we have demonstrated that sera withdrawn from mice injected with 5-nm or smaller GNPs showed binding activity against corresponding GNPs. However, the titers are approximately 1,000 which are at the lower boundary of positive binding. The administration of adjuvant did not affect the low frequency of obtaining antiserum with positive binding. Therefore, the low immunogenic binding activity of GNPs below 5-nm is insignificant compared to the antibody response against the synthetic peptide.

### **1.3.3 Antibody response of pFMDV-GNP conjugates is associated with the amount of GNPs taken up by Spleen**

The pFMDV-GNP conjugates could be taken up by antigen presenting cells (APCs) including macrophages and dendrite cells. Those APCs are transported through circulation to spleen. Epitopes on the surface of APCs are recognized by T cell, followed by subsequent T-cell activation to elicit an effective immune response. The presence and accumulation of pFMDV peptide-GNPs in spleen would ensure effective immunogenicity of the peptide.

The amount of pFMDV-GNPs in the spleen was evaluated by ICP-MS (**Figure1.11**). The pFMDV-GNPs showed size-dependent biodistribution in spleen. The distribution profile of pFMDV-GNPs in spleen shared a striking similarity with the antibody binding profile (**Figure 3-6**). The accumulation reached maximum for 12-nm GNP.

The ability of GNP to carry conjugated peptides into spleen seems to depend solely on the size of GNP. When the naked GNPs were injected into mice, the biodistribution of GNPs in spleen showed almost identical profile with pFMDV-GNPs conjugates (**Figure1.12**). The similarity indicated that surface modification of GNP did not alter the ability of GNP entering spleen. It also demonstrated the size-dependent invading ability of GNPs. Conjugation of pFMDV apparently enhanced the ability of GNPs to invade and accumulate in spleen regardless the size of GNPs.

Transmission electron microscopy (TEM) was performed to verify the presence of GNPs in the spleen (**Figure 1.12**). GNPs of sizes from 2-nm to 50-nm were trapped in vesicles of the spleen. The number of GNPs trapped in the vesicles is minimal for 2-nm and 5-nm, maximizes for 8-nm and 12-nm, and decreases for 17 to 50-nm GNPs. The result from TEM is consistent with the distribution profile of ICP-MS.

The amount of GNPs accumulated in spleen is size-dependent, as evaluated by ICP-MS and TEM. The profile of accumulation matches the profile of immune response.

It has been reported endocytosis is dependent on the size of GNPs. GNPs enter cells in a size- and shape-dependent manner [28, 29]. The endocytosis of GNPs reaches a maximum when the size nears 50 nm, but GNPs released from the cells exhibited a linear relationship to size. It induced larger GNPs tend to accumulate in the cells. It is possible that the majority of injected GNPs are absorbed at the site of injection [40]. The slow release of larger particles causes the reduced amount of larger particles in blood circulation. The concentration of GNP in circulation maximizes at 8 to 12-nm [31, 33]. Therefore, the size-dependent accumulation in spleen could be due to difference of GNP concentration in blood.

In control experiment, unmodified GNPs also exhibited the same size-dependent distribution, and the amount of pFMDV-GNPs conjugates is higher than unmodified GNPs. It indicated that the peptide modification enhanced the uptake of APCs, and the accumulation in the spleen.



Here we show that size-dependent immunogenic property is associated with the amount of GNPs taken up by Spleen. The GNPs ranging from 8-nm to 17-nm may serve as ideal carrier to elicit focused antibody response against a synthetic peptide.

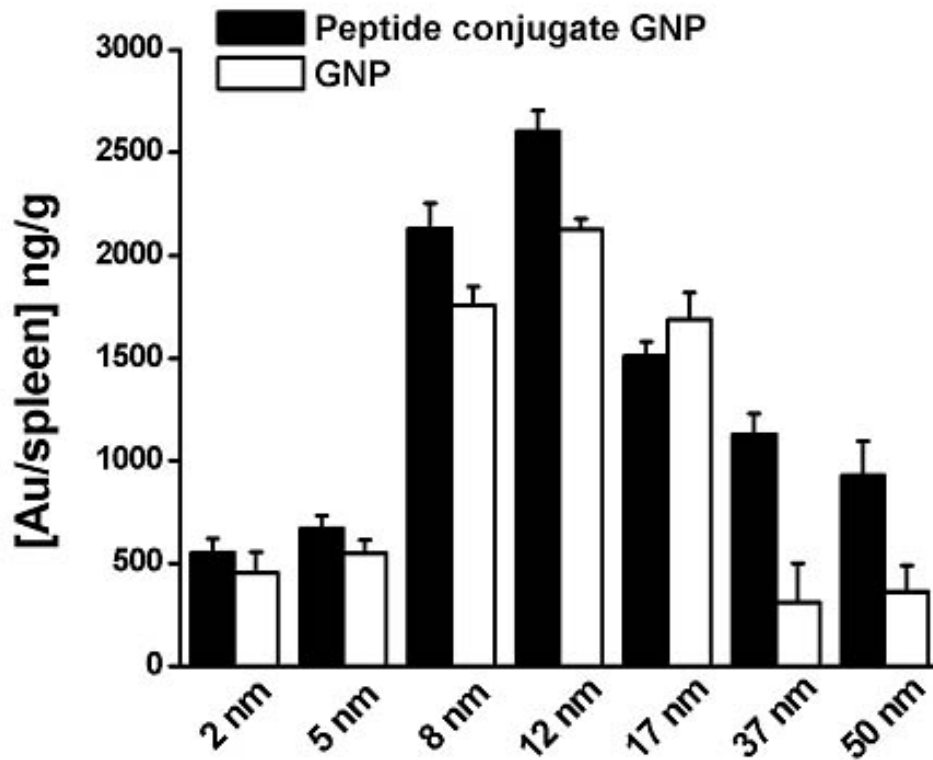


**Figure 1.11** Distribution of GNPs in mouse spleen. The pFMDV-GNP-injected mice are sacrificed at the end of the immunizing experiment. Amounts of GNPs in spleen are quantified by ICP-MS. Mice injected with pFMDV-GNPs are shown in filled columns. Unmodified GNPs are also injected and the biodistribution are shown in empty columns. The values are averaged from six mice.

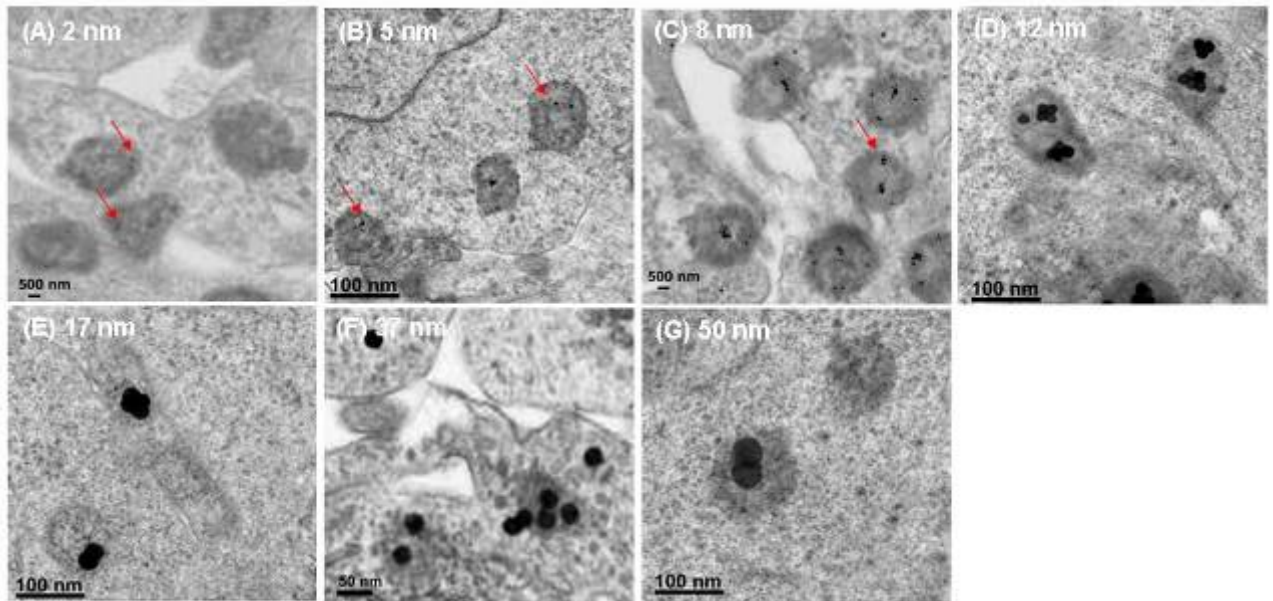


**Figure 1.12** TEM images of spleen obtained from pFMDV-GNPs-injected mice. Mice are injected with pFMDV-GNPs of various GNP diameters at: (A) 2-nm GNP, (B) 5-nm GNP, (C) 8-nm GNP, (D) 12-nm GNP, (E) 17-nm GNP, (F) 37-nm GNP, and (G) 50-nm GNP. The arrows indicate the aggregation and accumulation of GNPs in the vesicles of spleen cells.



## 1.4. Conclusion

We evaluated the potential application of gold nanoparticles as vaccine carrier. GNPs possess apparent advantages over KLH: pFMDV-GNPs induce ca 3.4-fold antibody response compared to pFMDV-KLH; GNPs alone do not induce immune response; and the conjugation of peptide-GNP is straightforward which requires additional incorporation of cysteine residue to the synthetic peptide.

The optimized size range of GNPs resides between 8-nm to 17-nm. This range of GNPs stimulated the highest levels of antibody response and also were accumulated the highest amount in the spleen.



# Reference

- [1] Grubman M J and Baxt B 2004 *Clin Microbiol Rev* **17** 465-93
- [2] Brooksby J B 1982 *Intervirology* **18** 1-23
- [3] Dunn C S and Donaldson A I 1997 *Vet Rec* **141** 174-5
- [4] Yang P C, Chu R M, Chung W B and Sung H T 1999 *Vet Rec* **145** 731-4
- [5] Bachrach H L 1968 *Annu Rev Microbiol* **22** 201-44
- [6] Acharya R, Fry E, Stuart D, Fox G, Rowlands D and Brown F 1989 *Nature* **337** 709-16
- [7] Carrillo C, Wigdorovitz A, Trono K, Dus Santos M J, Castanon S, Sadir A M, Ordas R, Escribano J M and Borca M V 2001 *Viral Immunol* **14** 49-57
- [8] Shieh J J, Liang C M, Chen C Y, Lee F, Jong M H, Lai S S and Liang S M 2001 *Vaccine* **19** 4002-10
- [9] Bittle J L, Houghten R A, Alexander H, Shinnick T M, Sutcliffe J G, Lerner R A, Rowlands D J and Brown F 1982 *Nature* **298** 30-3
- [10] Strohmaier K, Franze R and Adam K H 1982 *J Gen Virol* **59** 295-306
- [11] Hou Y and Gu X X 2003 *J Immunol* **170** 4373-9
- [12] May R J, Beenhouwer D O and Scharff M D 2003 *J Immunol* **171** 4905-12
- [13] van Houten N E, Zwick M B, Menendez A and Scott J K 2006 *Vaccine* **24** 4188-200
- [14] De Silva B S, Egodage K L and Wilson G S 1999 *Bioconjug Chem* **10** 496-501
- [15] Riemer A B, Klinger M, Wagner S, Bernhaus A, Mazzucchelli L, Pehamberger H, Scheiner O, Zielinski C C and Jensen-Jarolim E 2004 *J Immunol* **173** 394-401
- [16] Rubinchik E and Chow A W 2000 *Vaccine* **18** 2312-20
- [17] Maitta R W, Datta K, Lees A, Belouski S S and Pirofski L A 2004 *Infect Immun* **72** 196-208
- [18] Beenhouwer D O, May R J, Valadon P and Scharff M D 2002 *J Immunol* **169** 6992-9

- [19] Fan J, Liang X, Horton M S, Perry H C, Citron M P, Heidecker G J, Fu T M, Joyce J, Przysiecki C T, Keller P M, Garsky V M, Ionescu R, Rippeon Y, Shi L, Chastain M A, Condra J H, Davies M E, Liao J, Emini E A and Shiver J W 2004 *Vaccine* **22** 2993-3003
- [20] Tompkins S M, Zhao Z S, Lo C Y, Mispelon J A, Liu T, Ye Z, Hogan R J, Wu Z, Benton K A, Tumpey T M and Epstein S L 2007 *Emerg Infect Dis* **13** 426-35
- [21] Paciotti G F, Myer L, Weinreich D, Goia D, Pavel N, McLaughlin R E and Tamarkin L 2004 *Drug Deliv* **11** 169-83
- [22] Loo C, Lin A, Hirsch L, Lee M H, Barton J, Halas N, West J and Drezek R 2004 *Technol Cancer Res Treat* **3** 33-40
- [23] Pissuwan D, Valenzuela S M and Cortie M B 2006 *Trends Biotechnol* **24** 62-7
- [24] Tomii A and Masugi F 1991 *Jpn J Med Sci Biol* **44** 75-80
- [25] Dean H J, Fuller D and Osorio J E 2003 *Comp Immunol Microbiol Infect Dis* **26** 373-88
- [26] Dykman L A, Sumaroka M V, Staroverov S A, Zaitseva I S and Bogatyrev V A 2004 *Izv Akad Nauk Ser Biol* 86-91
- [27] Vasilenko O A, Staroverov S A, Yermilov D N, Pristensky D V, Shchyogolev S Y and Dykman L A 2007 *Immunopharmacol Immunotoxicol* **29** 563-8
- [28] Chithrani B D, Ghazani A A and Chan W C 2006 *Nano Lett* **6** 662-8
- [29] Chithrani B D and Chan W C 2007 *Nano Lett* **7** 1542-50
- [30] Hauck T S, Ghazani A A and Chan W C W 2008 *Small* **4** 153-9
- [31] De Jong W H, Hagens W I, Krystek P, Burger M C, Sips A J and Geertsma R E 2008 *Biomaterials* **29** 1912-9
- [32] Yu-Shiun Chen Y-C H, Ian Liau ,and G. Steve Huang 2009 *Nanoscale Res Lett*
- [33] Sonavane G, Tomoda K and Makino K 2008 *Colloids and Surfaces B-Biointerfaces* **66** 274-80

- [34] Brown K R, Walter D G and Natan M J 2000 *Chemistry of Materials* **12** 306-13
- [35] Liu F K, Ker C J, Chang Y C, Ko F H, Chu T C and Dai B T 2003 *Japanese Journal of Applied Physics Part 1-Regular Papers Short Notes & Review Papers* **42** 4152-8
- [36] Slot J W and Geuze H J 1985 *Eur J Cell Biol* **38** 87-93
- [37] Beekman N J, Schaaper W M, Turkstra J A and Melen R H 1999 *Vaccine* **17** 2043-50
- [38] Gharavi A E, Pierangeli S S, Colden-Stanfield M, Liu X W, Espinola R G and Harris E N 1999 *J Immunol* **163** 2922-7
- [39] Huang G S, Chen Y S and Yeh H W 2006 *Nano Lett* **6** 2467-71
- [40] Manolova V, Flace A, Bauer M, Schwarz K, Saudan P and Bachmann M F 2008 *Eur J Immunol* **38** 1404-13



# Chapter 2

## 2.1 introduction

### 2.1.1. General introduction to influenza A virus subtype H5N1

Influenza A virus subtype H5N1, also known as "bird flu. In general, avian influenza viruses do not replicate efficiently in humans, which suggests that direct transmission of an avian influenza virus to humans would be an extremely rare event, because high doses of avian influenza viruses are required to produce a quantifiable level of replication in human volunteers [1].

However, this perception changed in 1997, when an H5N1 highly pathogenic avian influenza virus was directly transmitted from birds to humans. In May 1997, an H5N1 virus was isolated from a 3-year-old boy in Hong Kong [2, 3], who later died of extensive influenza pneumonia complicated by Reye syndrome. By the end of 1997, 18 people had been infected by the virus, six of whom died. Humans who catch a humanized Influenza A virus usually have symptoms that include fever, cough, sore throat, muscle aches, conjunctivitis, and in severe cases, breathing problems and pneumonia that may be fatal. The severity of the infection depends to a large part on the state of the infected person's immune system and whether the victim has been exposed to the strain before [4] (in which case they would be partially immune). In August 2006, the World Health Organization (WHO) reported 240 confirmed human cases of H5N1 virus infection across ten countries, with 141 deaths (**Figure**

2.1).

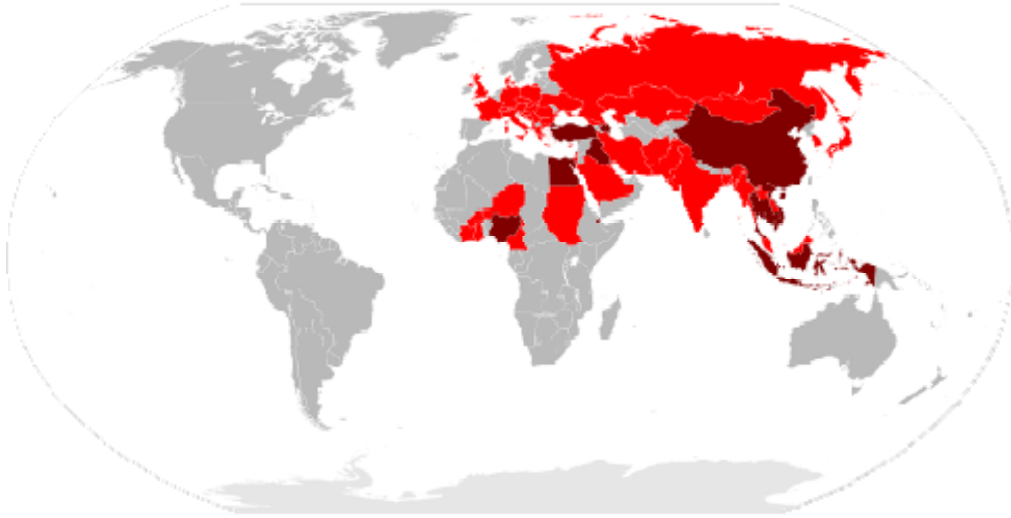
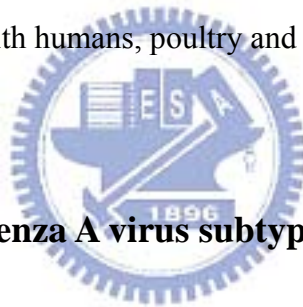


**Figure 2.1** The red color indicated countries with poultry or wild birds killed by H5N1, and the dark red indicated countries with humans, poultry and wild birds killed by H5N1 [4].



### 2.1.2. The structure of influenza A virus subtype H5N1

Three types of transmembrane proteins are expressed in the membrane of influenza type A virions and virus-infected cells: hemagglutinin (HA), neuraminidase (NA), and the third viral transmembrane protein, matrix protein 2 (M2), contains an ectodomain (M2e) that has remained highly conserved amongst human influenza virus strains (**Figure 2.2**). Many studies have highly interest in testing it for potential M2e-based peptide vaccine inducing broadly protective immunity against influenza type A virus infection maturation [5, 6].



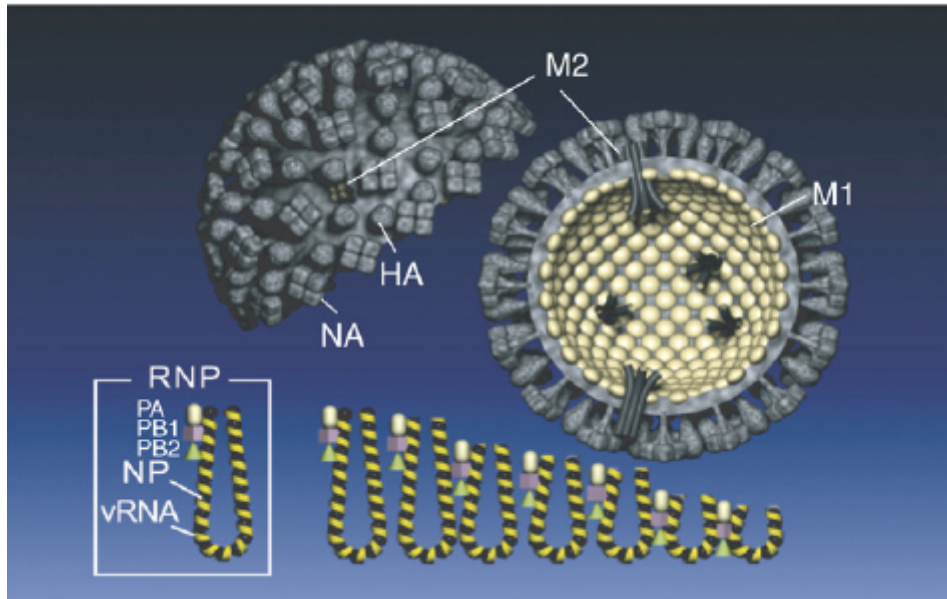


**Figure 2.2** Diagram of influenza A virion. Two glycoprotein spikes, HA and NA, and the M2 protein are embedded in the lipid bilayer derived from the host plasma membrane [4].



M2e-based peptide vaccine including the conserved M2 ectodomain peptide (23 amino acids) of type A viruses is immunized with a carrier molecule. Although preclinical trials using animal models indicate that these strategies might be safe and effective as vaccines, it is not known whether they provide any protection in humans.

### 2.1.3. Peptide Vaccine

Synthetic peptides have been applied as vaccines in recent years; however carriers are needed for efficient immune response. Peptides are generally not immunogenic enough to elicit high levels of antibody response. To enhance the immune response, peptides are coupled to carrier molecules to form peptide-carrier constructs. Large proteins or toxoids are regularly

used as carriers, such as keyhole limpet hemocyanin (KLH) [7, 8], ovalbumin (OVA) [9, 10], bovine serum albumin (BSA) [11, 12], and tetanus toxoid (TT) [13, 14]. Moreover, this kind of peptide vaccine technology has been widely used in influenza [15, 16] or other disease [17] vaccines recently.

Most carriers currently in use are not ideal. Some carrier proteins elicit strong antibody responses and suppress immune-response of peptide. For biological compounds, only few conjugation sites are available, leading to insufficient presentation of epitope and most important of all also exposing unnecessary antigenic sites of carriers themselves. Many carrier proteins are not stable in solution and conjugation between carrier protein and peptide often results in precipitates, causing non-reproducible conjugation and complicated analysis of end products. The major drawbacks indicate the need for improved carrier molecules.



#### **2.1.4. The advantage of gold nanoparticle served as vaccine carrier**

To serve as a general carrier, basic parameters such as the toxicity, immunogenicity, and specificity need to be characterized. Gold nanoparticles (GNPs) have been previously applied as immunogenic carriers such as drug delivery [18], cancer cell imaging [19], and photo-activated therapeutic [20], and as antigen carrier for the antibody generation [21-24]. GNPs possess many advantages as vaccine carrier. Synthesis of GNPs has been studied for decades and the reaction is well known and the wet chemistry is easy to operate in laboratory.

GNP is synthesized as a specific size which is controlled by the reaction conditions. GNPs are stable in solution. The aggregation of GNPs causes color change and can be traced visually. Gold is one of the best biocompatible materials. Gold has unusual affinity to sulfhydryl group, thus tight conjugation to peptide is achieved by the addition of extra cysteine residue to the peptide. However, as a general vaccine carrier, the in vivo toxicity, immunogenicity, and specificity, and most important of all, the size dependency of GNPs is not clear at the present time.

### **2.1.5. Motivation**

The purpose of this study is to investigate the potential role of gold nanoparticles as vaccine carrier. Immunogenicity and specificity was evaluated using KLH as control. Particularly, size has been played a pivotal role in the endocytosis and toxicity of GNPs to cells [25-27] and animals [28-30]. It is foreseeable that size may play an important role for GNPs as a vaccine carrier.



## 2.2: Experiment and Method

### 2.2.1. Chemicals

HAuCl<sub>4</sub>, sodium citrate, NaBH<sub>4</sub>, HCl, HNO<sub>3</sub>, H<sub>2</sub>SO<sub>4</sub>, H<sub>2</sub>O<sub>2</sub>, and other chemicals of analytical grade were purchased from Sigma-Aldrich and Fisher. H<sub>2</sub>O was >18 MΩ from a Milli-Q water purification system.

### 2.2.2. Preparation and characterization of gold nanoparticle

Gold nanoparticles (GNPs) of diameter with 2-nm, 5-nm, 8-nm, 12-nm, 17-nm, 37-nm, and 50-nm were synthesized as reported previously [31, 32]. The seed colloids were prepared by adding 1 mL of 0.25 mM HAuCl<sub>4</sub> to 90 mL of H<sub>2</sub>O and stirred for 1 min at 25 °C. Two milliliters of 38.8 mM sodium citrate were added to the solution and stirred for 1 min, followed by the addition of 0.6 mL of freshly prepared 0.1 M NaBH<sub>4</sub> in 38.8 mM sodium citrate. Different diameters of GNPs ranging from 3 nm to 100 nm were generated by changing the volume of seed colloid added. The solution was stirred for an additional 5-10 min at 0-4 °C. Reaction temperatures and times were adjusted to obtain GNPs of larger size. All synthesized GNPs were characterized by UV absorbance. The size of synthesized GNPs was verified by electron microscopy and atomic force microscopy. GNPs were dialyzed against phosphate-buffered saline (pH 7.4) before injection into the animals.

### **2.2.3. Designing of Synthetic peptide**

The highly immunogenic peptides pFMDV and pH5N1 were designed and synthesized based on viral protein 1 of foot-and-mouth disease virus type O and matrix protein 2 of influenza A virus A/Hong Kong/482/97 H5N1, respectively. The amino acid sequences are NGSSKYGDTSTNNVRGDLQVLAQKAERTLC for pFMDV and MSLLETVETLTRNGW GCRCSDSSDC for pH5N1. An extra cysteine was added to the C-terminus of each peptide in order to improve binding to the gold surface.

### **2.2.4. Preparation of pH5N1-carrier conjugates**

For preparing KLH conjugates, were synthesized as reported previously [15, 16] , pH5N1 containing cysteine was resuspended in Milli-Q water at 1 mg/ml, and the pH was adjusted to approximately 8.5 by addition of dilute NaOH. Commercial maleimide-activated KLH (Pierce. ALEX, IL) was reconstitute in 50mM sodium phosphate, 0.15M NaCl, 0.1M EDTA, pH 7.2 buffer at 10 mg/ml. Peptide and carrier were mixed at a 0.5 molar ratio of thiol to maleimide in 0.1M sodium phosphate, 0.15M NaCl, 10mM EDTA, pH 7.2 buffer and allowed to react in the dark at 25 °C. The conjugated complexes were purified by centrifugation and resuspended in PBS to final concentration (0.01 ug/ul). The conjugate was separated from unreacted peptide and carrier by HPLC.

For preparing Gold nanoparticle conjugates, the approach used to conjugate the gold

nanoparticles with peptide was based on titration methods [33]. An extra cysteine was added to the C-terminus of each peptide in order to improve binding to the gold surface. Conjugation of antigen with GNPs was performed by titration the antigens into a GNP solution. The titration was monitored by UV absorption at the wavelength appropriate for each peptide to detect aggregation of unsaturated GNP in the presence of 1 M sodium chloride. After reaching the saturation point, the conjugated complexes were purified by centrifugation and resuspended in PBS to final concentration (0.01 ug/ul)

### **2.2.5. Immunization of mice**

Animal treatments were performed following “The Guidelines for the Care and Use of Experimental Animals” of National Chiao Tung University. Four-week-old male BALB/C mice were housed at  $22\pm 2$  °C with a 12-h light/dark cycle and fed standard rodent chow and water ad libitum. Mice were randomly assigned to experimental groups. Each group consisted of 6 mice.

Groups of 4-week-old BALB/c mice were given intraperitoneal (IP) and subcutaneous (SC) immunizations with: (1) pH5N1-KLH conjugate and (2) pH5N1-GNPs conjugates with sizes of 2-nm, 5-nm, 8 nm, 12-nm, 17-nm, 37-nm and 50-nm. Those antigens were administered with equal volume of complete and incomplete adjuvant.

For all groups, the mice were immunized on week 0, 1, 2, 3, 5, 7 and 9, and the blood

was collected from tail vein after week 4, 6, 8, and 10. The sera were collected after centrifugation and stored at  $-20^{\circ}\text{C}$ . Animals were sacrificed at the end of experiment by cardiac puncture under  $\text{CO}_2$  anaesthesia. The spleens were isolated and organ weights of all mice were measured.

### **2.2.6 Enzyme-linked immunosorbent assay (ELISA)**

In order to coat wells with GNP as an antigen, each microwell of a 96-well Corning plate was pre-treated with 200  $\mu\text{L}$  of 1 mM 3-aminopropyl-triethoxysilane (APTES) in ethanol at room temperature for 40 min. The activated wells were washed with ethanol twice for 5 min, followed by distilled water for 5 min. Gold nanoparticles (15mM, 150uL) were added to the microwells and incubated for 2 h at room temperature, followed by three Milli-Q water washes and finally with three washes with 0.5% Triton X-100 in PBS. To coat wells with other antigens, 100  $\mu\text{L}$  of antigen was added into microwells and incubated at room temperature for 30 min, followed by three PBS washes. Blocking for non-specific binding was performed by adding 100  $\mu\text{L}$  of 3% BSA and incubating for 60 min at room temperature, followed by three PBS washes. Binding was performed by adding 100  $\mu\text{L}$  of diluted antiserum into microwells and incubating for 1 hr at room temperature, followed by thorough washes. HRP-conjugate anti-mouse IgG, 2,2'-azino-di-(3 ethylbenzthiazoline sulfonic acid)

(ABTS) and H<sub>2</sub>O<sub>2</sub> were added in sequence to the wells according to the manufacturer's protocol, and the binding efficiency was monitored by measuring absorbance at 405 nm.

### **2.2.7 Inductively coupled plasma mass spectrometry (ICP-MS)**

For the total elements determinations, standard solutions were prepared by dilution of a multi-element standard (1,000 mg L<sup>-1</sup> in 1 M HNO<sub>3</sub>) obtained from Merck (Darmstadt, Germany). Nitric acid (65%), hydrochloric acid (37%), perchloric acid (70%), and hydrogen peroxide (30%) of Suprapur® grade (Merck) were used to mineralize the samples. A size-exclusion column was connected to the ICP-MS apparatus. Spleen section samples were homogenized in 25 mM tris (hydroxymethyl) aminomethane (Tris)–12.5 mM HCl buffer solution at pH 8 and centrifuged at 13,000 rpm for 1 h. The supernatant was applied to the size-exclusion column of the HPLC system, which had been equilibrated with 25 mM Tris–12.5 mM HCl (containing 20 mM KCl), and eluted with the same buffer at a flow rate of 1 mL/min. The metal components of metal-binding proteins that were eluted from the HPLC system were detected by ICP-MS (Perkin Elmer, SCIEX ELAN 5000). The main instrumental operating conditions were as follows: RF power 1900 W, carrier gas flow 0.8 L/min Ar and makeup gas flow 0.19 L/min Ar. The following isotopes were measured: <sup>197</sup>Au as internal standard.



### 2.2.8. Statistical Analyses

All data are presented as means  $\pm$  S.E.M. with a minimum of six mice in each group.

Concentrations of biogenic amines and Ach in spleen were analyzed using the unpaired student *t*-test. The criterion for statistical significance was  $p < 0.05$  for all statistical evaluations.



## 2.3: Result and Discussion

### 2.3.1. Preparation and analysis of pH5N1 peptide and Gold nanoparticle conjugates

To further investigate the utility of GNPs as vaccine carrier, pH5N1 was designed and synthesized based on the immunogenic epitope previously reported [15, 16]. In particular, an extra cysteine residue was attached to the C-terminus of the peptide to provide sulfhydryl group as conjugating site with GNPs. The pH5N1 was conjugated to GNPs of various sizes (2-nm, 5-nm, 8-nm, 12-nm, 17-nm, 37-nm and 50-nm). Synthesis of GNPs with varied sizes was monitored by UV absorbance (**Figure 2.3**) and examined by electron microscopy (**Figure 2.4**). Conjugation of pH5N1-GNP was optimized by NaCl-induced aggregation [33]. The lowest concentration of peptide that did not cause a color change from red to dark blue was chosen for conjugation.

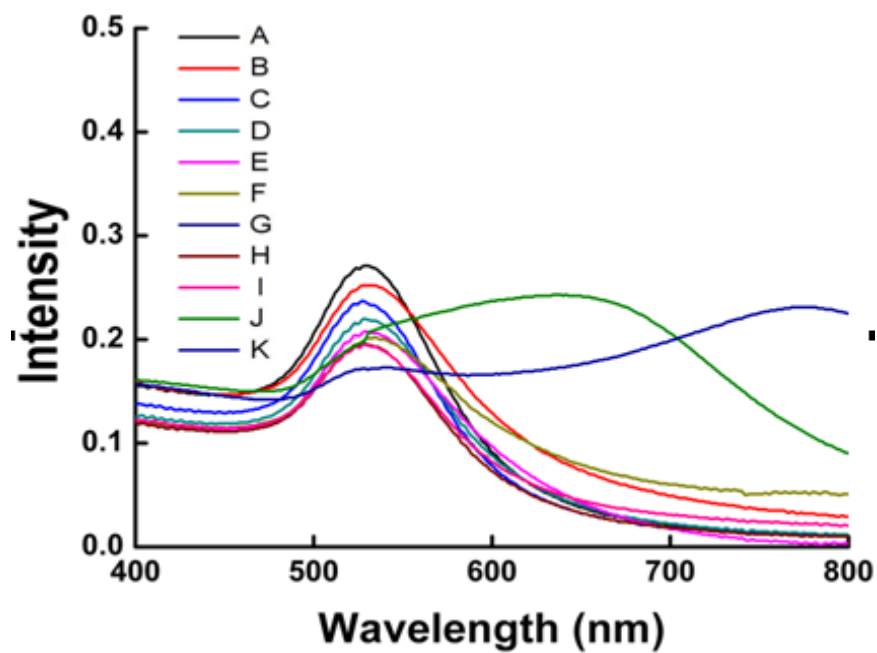



**Figure 2.3** UV-Vis absorbance measurements of GNPs with shift of the surface plasmon band peaks correlating with peptide of different concentrations.

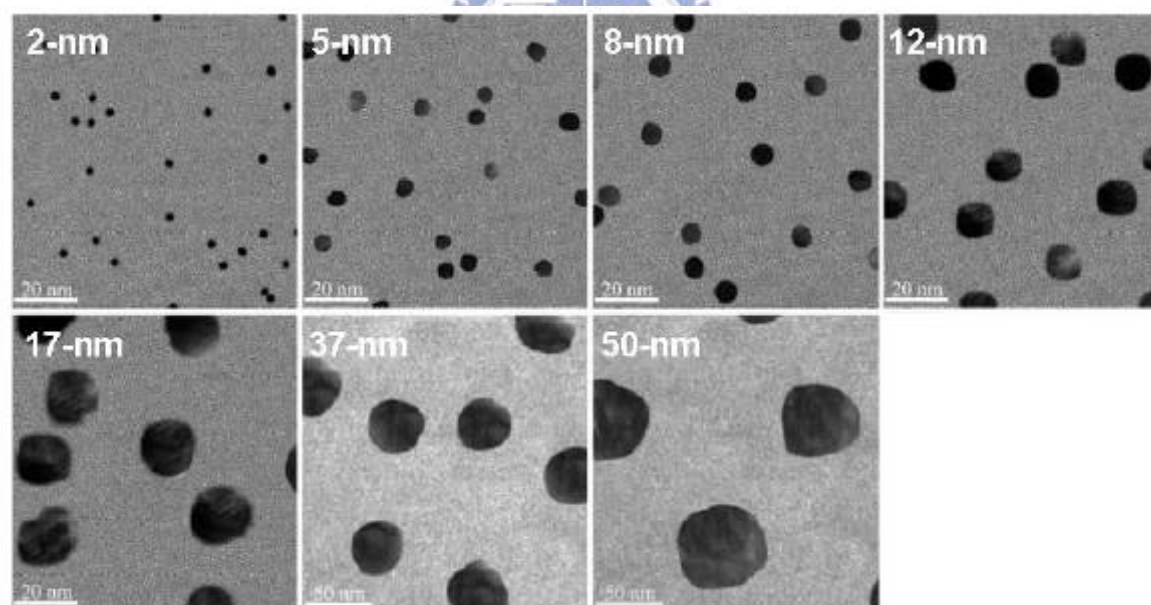


**Figure 2.4** TEM images for the GNPs synthesized in the current study. GNPs with diameters of 2-nm, 5-nm, 8-nm, 12-nm, 17-nm, 37-nm, and 50-nm were examined under an electron microscope. Scale bars are 20-nm for images of 2-nm, 5-nm, 8-nm, 12-nm, and 17-nm GNPs. Scale bars are 50-nm for images of 37-nm, and 50-nm GNPs.

### **2.3.2. The pH5N1-GNP conjugates induced focused and enhanced antibody response**

Mice were immunized with pH5N1-GNP conjugates with varied sizes of GNPs. Each injection contains equal amount of pH5N1-GNP (The final concentration is  $0.01 \mu\text{g}/\mu\text{l}$ ). For control experiment, mice were injected with pH5N1-KLH (The final concentration is  $0.01 \mu\text{g}/\mu\text{l}$ ). These conjugates were injected intraperitoneally and subcutaneously into BALB/C mice weekly from week 0. Tail blood was withdrawn at week 4, 6, 8, and 10. ELISA was performed to obtain titers of antisera against pH5N1, GNPs, and KLH (**Figure 2.5 and Figure 2.6**).



Significant antibody response appeared for antisera withdrawn on week 6 (**Figure 2.5A**). The binding affinity using pH5N1 as antigen showed a size-dependent profile. The pH5N1-2-nm GNP induced titer of  $60,000 \pm 1700$  at week 10 (**Figure 2.5B**). The induced titers increased when the size of GNPs increased, maximized at 8 nm of  $112,300 \pm 1900$ , and decreased to 0 for 50-nm GNP. The pH5N1-KLH conjugate induced antibody response with titer of  $51200 \pm 1230$ . Binding activity of antisera withdrawn from week 10 mice elicited binding profile comparable to week 6. However, pH5N1-GNP conjugates induced higher immune response than pH5N1-KLH. A 2.17-fold enhancement of antibody response occurred to 8-nm GNP compared to the use of KLH as carrier.

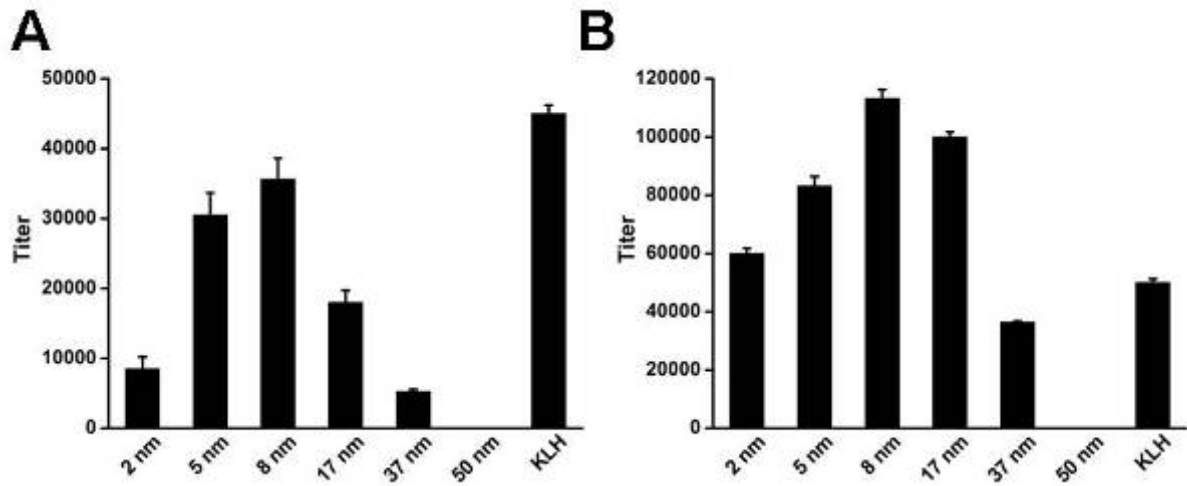


**Figure 2.5** Titers of antiserum withdrawn from pH5N1-GNPs injected mice on (a) sixth week and (b) tenth week of immunizations against pH5N1. The values are averaged from 6 independent mice. Titer of pH5N1-KLH serves as control. Sera obtained from pH5N1-37-nm GNP and pH5N1-50-nm GNP injected mice do not show detectable binding activity.

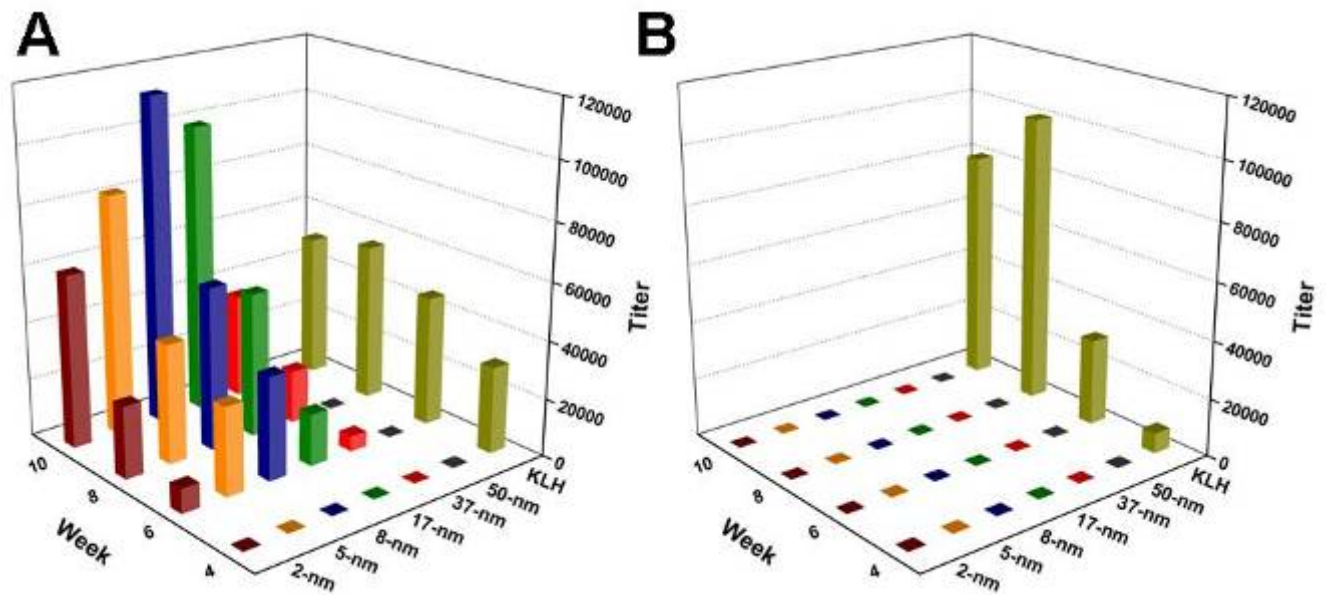


**Figure 2.6** Titers of antisera withdrawn from pH5N1-GNPs injected mice on week 4, 6, 8 and 10. The antigens used in the ELISA are (A) pH5N1 (B) GNPs/KLH. Titers of pH5N1-KLH are incorporated as control.

When overall antibody responses of week 4, 6, 8, and 10 were compared, a size-dependent tendency was observed (**Figure 2.6A**). GNPs (ranging from 2-nm to 8-nm) exhibited increasing binding affinity following subsequent immunizations. Highest binding activity occurred at 8-nm GNP. Gradual decrease in titer was observed for 17-nm and 37-nm GNPs. We could not observe induced binding activity for 50-nm GNP conjugates until the end of experiment. KLH conjugate remained medium binding affinity compared to GNP conjugates.

Antibody response to the carrier is an important parameter which determines the focused immunogenicity of the conjugated peptide. An ideal carrier should remain silent during the immunization of peptide conjugates. KLH and other carriers are known to induce significant immune response [34, 35, 8]. The binding activity of antiserum against KLH was observed from week 4 and increased to a significant level of  $81,000 \pm 2700$  on week 10 (**Figure 2.6B**). On the contrary, GNPs regardless of the size showed no detectable binding activity during the course of our experiment.

It was reported that KLH conjugate exhibits strong immune response. KLH also exhibits non-specifically binding to the antigen and give rise to false positive binding of cross reactivity. KLH as a carrier exhibited high immune response against itself with the titer even higher than anti-pH5N1 (**Figure 2.6**). It is likely that conjugation of pH5N1 with KLH generated potent recognition sites, thus complicated the induced antibody species. The

antibodies strongly recognize pH5N1-KLH conjugates and KLH. Antibody populations that specifically bind to synthetic pH5N1 are greatly reduced.

Compared to KLH carrier, GNPs as a carrier exhibit undetectable antibody response. However, when conjugated with pH5N1-GNP showed strong antibody response against pH5N1. Conjugation to carrier does not altered antibody response against synthetic pH5N1.

The result indicated that antibody response to pH5N1-GNPs selectively resided and focused on the conjugated peptide (**Figure 2.7**), while antibodies responding to pH5N1-KLH treated KLH as additional immune targets. GNPs are demonstrated to be ideal candidates as vaccine carrier for their inert to immune system.

Here we show GNPs as excellent vaccine carriers. Comparing to KLH GNPs exhibited approximately 2.17-fold enhancement of immunogenicity and apparently no detectable binding activity to themselves. Thus GNPs displayed all characteristics for an ideal vaccine carrier.

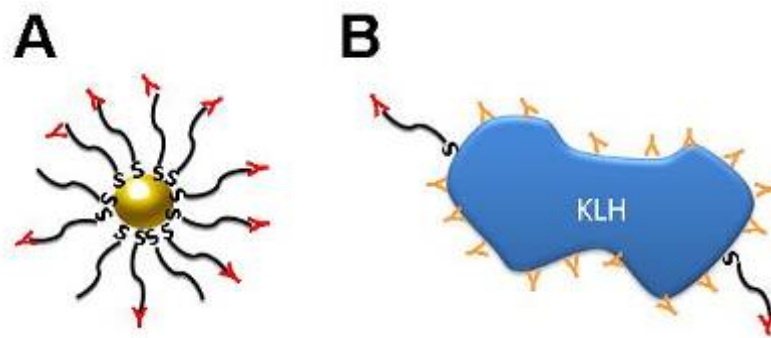
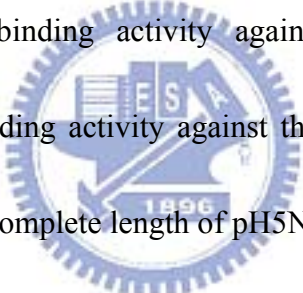


**Figure 2.7** (A) The antibody focused recognizes the pH5N1 adsorbed on surface of GNPs (B)

The antibody recognizes both pH5N1 and KLH so that reduce the binding activity of pH5N1.

### 2.3.3. The anti-pH5N1 antiserum recognized whole pH5N1 as epitope

Further examination to the sequence of peptide we found cysteine residues at the 17th and 19th position of the pH5N1. It is very like that all 3 cysteines are bound to the gold surface leaving 16 amino acid residues stem into solution. It is possible that antibody thus generated recognized against these 16 amino acid residues. To verify this hypothesis, a shorter version containing this 16 amino acid peptide was synthesized (pSH5N1, **Table 2.1**). We also synthesized a longer version with extra 5 glycine residues at the N-terminus of pH5N1 (pLH5N1). The pH5N1-generated antiserum exhibited the highest titers against pH5N1 ( $110,000 \pm 2200$  at 8-nm), low binding activity against the longer version (pLH5N1,  $10,090 \pm 700$  at 8-nm), and no binding activity against the short version (pSH5N1) (**Figure 2.8**). The result indicated that the complete length of pH5N1 was included in the epitope.



Synthesis peptide	Sequence
pH5N1	MSLLTEVETLTRNGWGCRCS DSSD(C)
pSH5N1	MSLLTEVETLTRNGWG(C)
pLH5N1	(C)GGGGGMSLLTEVETLTRNGWGCRCS DSSD

**Table 2.1** Sequence of synthesis different pH5N1



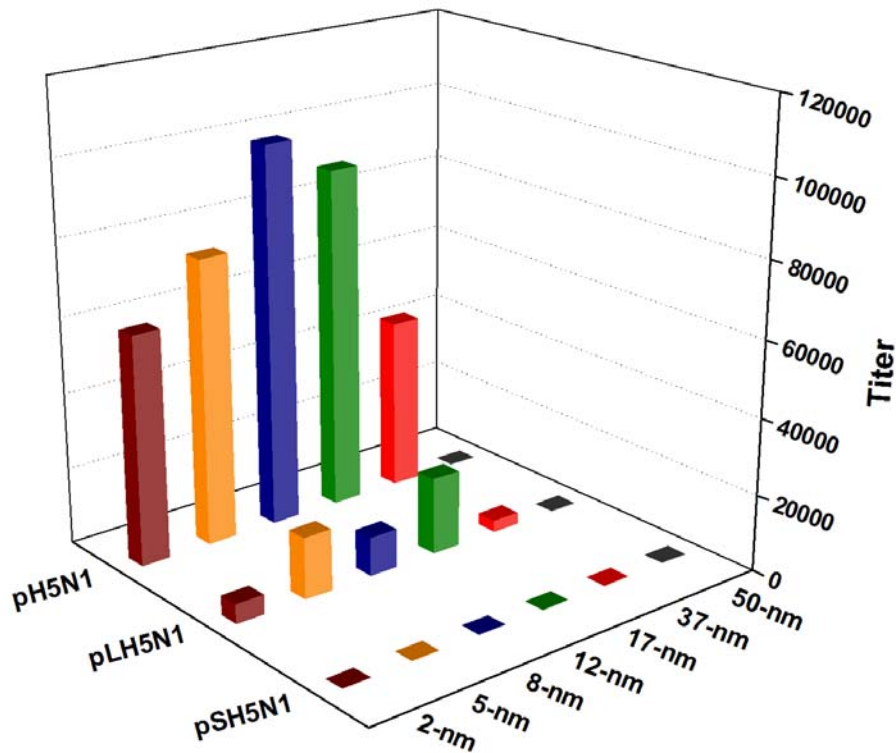


**Figure 2.8** The antibody response to pH5N1-GNPs selectively resided and focused on the conjugated peptide (pH5N1, pLH5N and pSH5N1).



### 2.3.4. Antibody response of pH5N1-GNP conjugates is associated with the length of peptide

To investigate the association between the length of peptide and immunogenicity, pSH5N1 and pLH5N1, were conjugated to GNPs of various sizes (2-nm, 5-nm, 8-nm, 17-nm, 37-nm and 50-nm) and injected into mice. Blood was withdrawn on each week and the titers against peptides were examined by ELISA (**Figure 2.9**).

Both pLH5N1 and pSH5N1 showed a size-dependent profile of binding activity. The induced titers increased when the size of GNPs increased, maximized at 8 nm and decreased

to 0 for 50 nm. The titer of pLH5N1 maximized of  $132,000 \pm 1600$  at 8-nm (**Figure 2.9A**) GNP showed the best binding activity than other peptide:  $111,300 \pm 2900$  at 8-nm GNP for pH5N1 and  $95,000 \pm 1100$  at 8-nm GNP for pSH5N1 (**Figure 2.9B**) at week 10. The result indicated that antibody response of pH5N1-GNP conjugates is associated with the length of peptide.

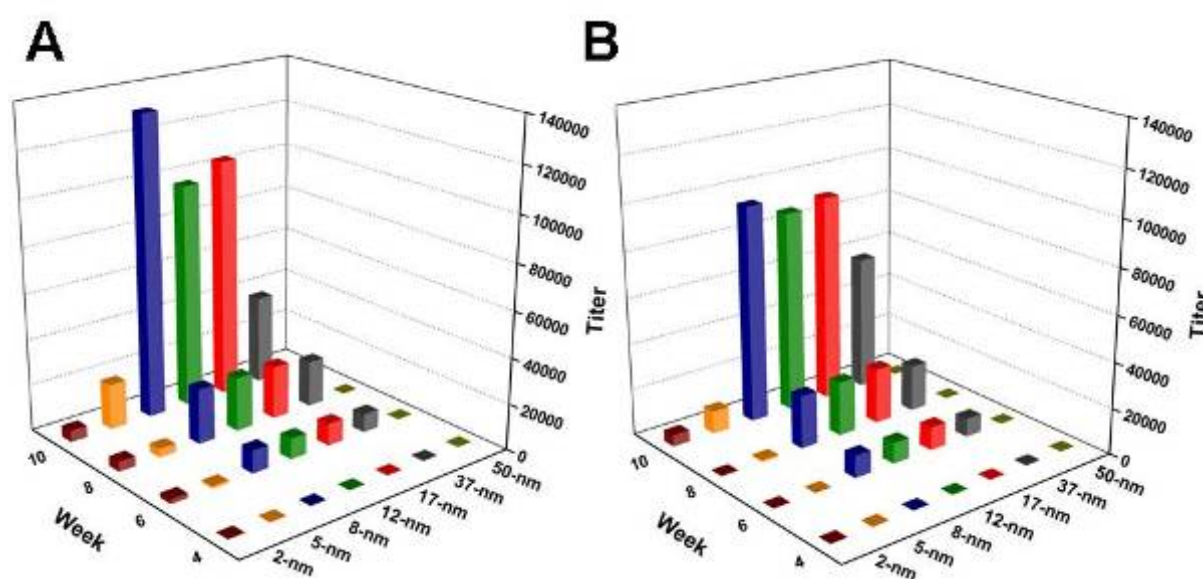


**Figure 2.9** Titers of antisera withdrawn from pLH5N1-GNPs and pSH5N1-GNPs injected mice on week 4, 6, 8 and 10. The antigens used in the ELISA are (A) pLH5N1 (B) pSH5N1

The generation of antibody from pLH5N1 and pSH5N1 not only showed a size-dependent profile (**Figure 2.6**), but also exhibited length-dependent (**Figure 2.9**). The induced titers increased when the length of peptide increased. Although pSH5N1 (16 amino acids) is sufficient to induce antibody response minimum length of peptide to induce significant immune response is dependent on the context of the peptide. We illustrated this

point of view by using various lengths of pFMDV-GNP conjugates.

### **2.3.5. Antibody response of pFMDV-GNP conjugates is associated with the length of peptide**

The ability of pSH5N1 (16 amino acids) to stimulate antibody response provided an opportunity to verify the general length rule for epitope. It is possible that GNPs were capable of presenting conjugated peptide regardless the minimum size for immunogenic peptide. To investigate if GNP is capable of reducing the required length of peptide, five peptides with different length were synthesized based on the amino acid residues 131–159 of VP1 of the foot and mouth disease virus (pFMDV-A, pFMDV-B, pFMDV-C, pFMDV-D, and pFMDV-E; **Table 2.2**) and conjugated to GNPs 8-nm and 12-nm GNPs [36, 37]. The conjugates were injected peritoneally into BALB/C mice weekly. Blood was withdrawn and the titers against their own peptides were examined by ELISA (**Figure 2.10**).

For 8-nm GNP as carrier, full length FMDV peptide (pFMDV, 25 a.a.) stimulated highest titer of  $40,000 \pm 1100$  on week 10. The titers dropped to  $8300 \pm 100$  for pFMDVD (20 a.a.),  $7800 \pm 400$  for pFMDVC, and to 0 for pFMDVB (10 a.a.) and 0 for pFMDVA (5 a.a.). For 12-nm GNP as carrier, full length FMDV peptide (pFMDV, 25 a.a.) stimulated highest titer of  $31100 \pm 1900$  on week 10. The titers dropped to  $4200 \pm 300$  for pFMDVD (20 a.a.),  $8700 \pm 670$  for pFMDVC, and to 0 for pFMDVB (10 a.a.) and 0 for pFMDVA (5 a.a.). The minimal length of peptide to stimulate immune response using GNP as carrier depends on the content

of the amino acid sequence. For pFMDV, a minimum of 25 amino acids is required.

Synthesis peptide	Sequence
pFMDV-A	ERTL(C)
pFMDV-B	LAQKAERTL(C)
pFMDV-C	GDLQVLAQKAERTL(C)
pFMDV-D	TNNVRGDLQVLAQKAERTL(C)
pFMDV	YGDSTNNVRGDLQVLAQKAERTL(C)

**Table 2.2** Sequence of synthesis different pFMDV

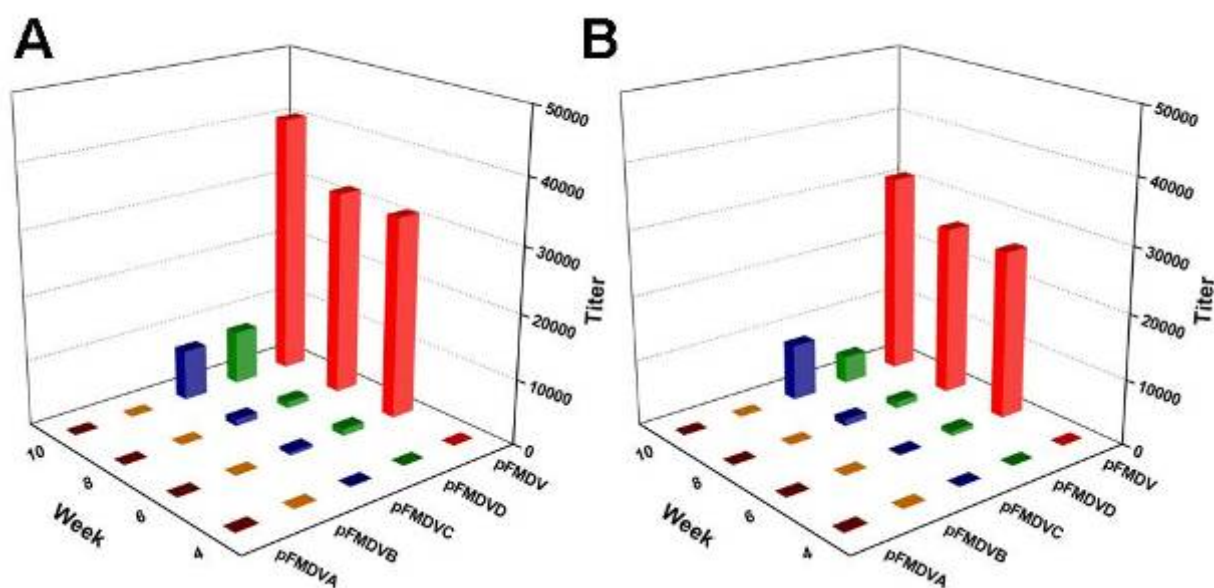
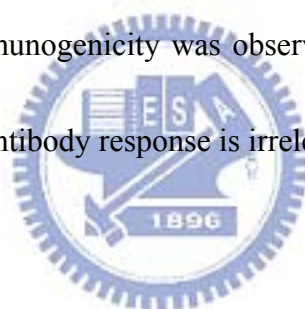


**Figure 2.10** Titers of antisera withdrawn from five different peptides with increasing number of amino acids (pFMDV-A, pFMDV-B, pFMDV-C, pFMDV-D, and pFMDV-E) and conjugated to GNPs (a) 8-nm and (b) 12-nm GNPs injected mice on week 4, 6, 8 and 10. The antigens used in the ELISA are own peptide.

Immunogenic conjugates are processed in spleen in order to generate antibody. The

difference in the ability of pFMDVs to generate antibody might be associated with the amount of GNPs deposited in spleen. The accumulation of GNP was analyzed by ICP-MS for the spleens isolated from mice injected with pFMDVs-8-nm GNP conjugates and pFMDVs-12-nm GNP conjugates (**Figure 2.11**). For 8-nm GNP conjugates, the concentration of gold element ranged from 1450 ng/g spleen to 1850 ng/g spleen. For 12-nm GNP conjugates, the concentration of gold element ranged from 1785 ng/g spleen to 2685 ng/g spleen. Unmodified gold exhibited comparable accumulation in either case. It indicated that surface modification of GNP did not alter the ability of GNP to enter spleen. No obvious correlation to the differential immunogenicity was observed. The minimal length of peptide conjugated on GNP to stimulate antibody response is irrelevant to their presence in spleen.



It is possible that the inability of shorter peptides to stimulate antibody response is due to inefficient transport into spleen. ICP-MS was performed to the spleens isolated from pFMDV-GNP conjugates (**Figure 2.11**). We found that surface modification of GNP did not alter the ability of GNPs entering spleen. The ability of peptide conjugates to stimulate antibody response is irrelevant to their presence in spleen.

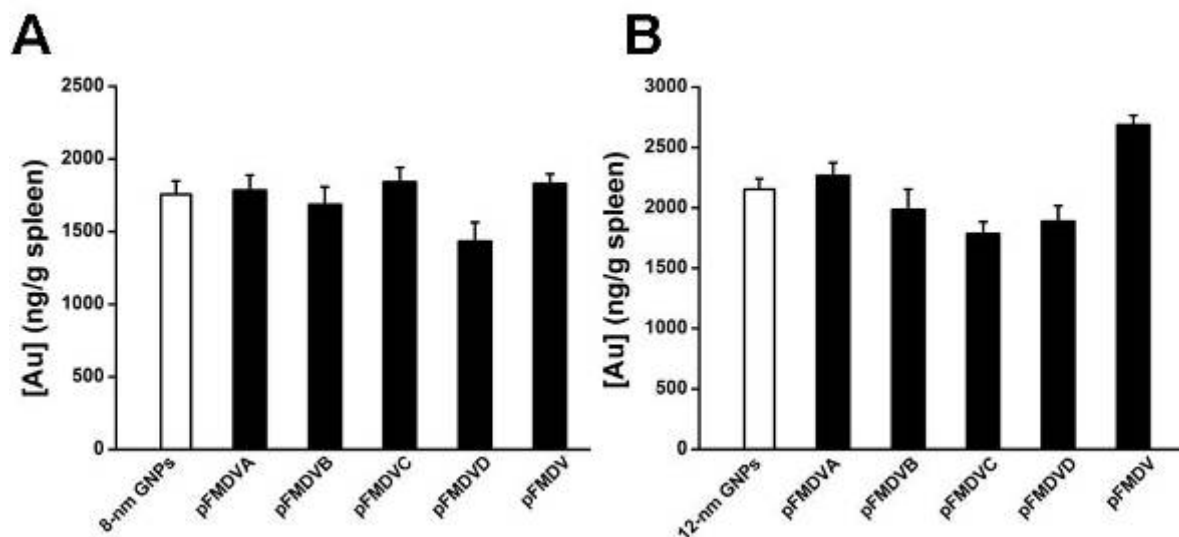
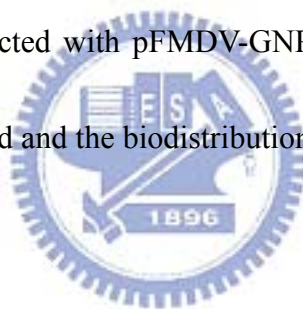


**Figure 2.11** Distribution of GNPs in mouse spleen. All pFMDV-GNP-injected mice are sacrificed at the end of the immunizing experiment. Amounts of GNPs in spleen are quantified by ICP-MS. Mice injected with pFMDV-GNPs type is shown in filled columns. Unmodified GNPs are also injected and the biodistribution are shown in empty columns.



## 2.5: Conclusion

We evaluated the potential application of gold nanoparticles as vaccine carrier. GNPs possess apparent advantages over KLH: pH5N1-GNPs induce ca 2-fold antibody response compared to pH5N1-KLH; GNPs alone do not induce immune response, thus the induced antibodies recognize peptide not carrier; and the conjugation of pH5N1-GNPs is straightforward which requires additional incorporation of cysteine residue to the synthetic peptide. The optimized size range of GNPs resides between 8-nm to 17-nm.



# Reference

- [1] Beare A S and Webster R G 1991 *Arch Virol* **119** 37-42
- [2] Horimoto T and Kawaoka Y 2005 *Nat Rev Microbiol* **3** 591-600
- [3] Subbarao K, Klimov A, Katz J, Regnery H, Lim W, Hall H, Perdue M, Swayne D, Bender C, Huang J, Hemphill M, Rowe T, Shaw M, Xu X, Fukuda K and Cox N 1998 *Science* **279** 393-6
- [4] Horimoto T and Kawaoka Y 2006 *Trends Mol Med* **12** 506-14
- [5] Neiryneck S, Deroo T, Saelens X, Vanlandschoot P, Jou W M and Fiers W 1999 *Nat Med* **5** 1157-63
- [6] Okuda K, Ihata A, Watabe S, Okada E, Yamakawa T, Hamajima K, Yang J, Ishii N, Nakazawa M, Ohnari K, Nakajima K and Xin K Q 2001 *Vaccine* **19** 3681-91
- [7] Hou Y and Gu X X 2003 *J Immunol* **170** 4373-9
- [8] May R J, Beenhouwer D O and Scharff M D 2003 *J Immunol* **171** 4905-12
- [9] van Houten N E, Zwick M B, Menendez A and Scott J K 2006 *Vaccine* **24** 4188-200
- [10] De Silva B S, Egodage K L and Wilson G S 1999 *Bioconjug Chem* **10** 496-501
- [11] Riemer A B, Klinger M, Wagner S, Bernhaus A, Mazzucchelli L, Pehamberger H, Scheiner O, Zielinski C C and Jensen-Jarolim E 2004 *J Immunol* **173** 394-401
- [12] Rubinchik E and Chow A W 2000 *Vaccine* **18** 2312-20
- [13] Maitta R W, Datta K, Lees A, Belouski S S and Pirofski L A 2004 *Infect Immun* **72** 196-208
- [14] Beenhouwer D O, May R J, Valadon P and Scharff M D 2002 *J Immunol* **169** 6992-9
- [15] Fan J, Liang X, Horton M S, Perry H C, Citron M P, Heidecker G J, Fu T M, Joyce J, Przysiecki C T, Keller P M, Garsky V M, Ionescu R, Rippeon Y, Shi L, Chastain M A,



- Condra J H, Davies M E, Liao J, Emini E A and Shiver J W 2004 *Vaccine* **22** 2993-3003
- [16] Tompkins S M, Zhao Z S, Lo C Y, Misplon J A, Liu T, Ye Z, Hogan R J, Wu Z, Benton K A, Tumpey T M and Epstein S L 2007 *Emerg Infect Dis* **13** 426-35
- [17] Shieh J J, Liang C M, Chen C Y, Lee F, Jong M H, Lai S S and Liang S M 2001 *Vaccine* **19** 4002-10
- [18] Paciotti G F, Myer L, Weinreich D, Goia D, Pavel N, McLaughlin R E and Tamarkin L 2004 *Drug Deliv* **11** 169-83
- [19] Loo C, Lin A, Hirsch L, Lee M H, Barton J, Halas N, West J and Drezek R 2004 *Technol Cancer Res Treat* **3** 33-40
- [20] Pissuwan D, Valenzuela S M and Cortie M B 2006 *Trends Biotechnol* **24** 62-7
- [21] Tomii A and Masugi F 1991 *Jpn J Med Sci Biol* **44** 75-80
- [22] Dean H J, Fuller D and Osorio J E 2003 *Comp Immunol Microbiol Infect Dis* **26** 373-88
- [23] Dykman L A, Sumaroka M V, Staroverov S A, Zaitseva I S and Bogatyrev V A 2004 *Izv Akad Nauk Ser Biol* 86-91
- [24] Vasilenko O A, Staroverov S A, Yermilov D N, Pristensky D V, Shchyogolev S Y and Dykman L A 2007 *Immunopharmacol Immunotoxicol* **29** 563-8
- [25] Chithrani B D, Ghazani A A and Chan W C 2006 *Nano Lett* **6** 662-8
- [26] Chithrani B D and Chan W C 2007 *Nano Lett* **7** 1542-50
- [27] Hauck T S, Ghazani A A and Chan W C W 2008 *Small* **4** 153-9
- [28] De Jong W H, Hagens W I, Krystek P, Burger M C, Sips A J and Geertsma R E 2008 *Biomaterials* **29** 1912-9
- [29] Yu-Shiun Chen Y-C H, Ian Liau ,and G. Steve Huang 2009 *Nanoscale Res Lett*
- [30] Sonavane G, Tomoda K and Makino K 2008 *Colloids and Surfaces B-Biointerfaces* **66** 274-80

- [31] Brown K R, Walter D G and Natan M J 2000 *Chemistry of Materials* **12** 306-13
- [32] Liu F K, Ker C J, Chang Y C, Ko F H, Chu T C and Dai B T 2003 *Japanese Journal of Applied Physics Part 1-Regular Papers Short Notes & Review Papers* **42** 4152-8
- [33] Slot J W and Geuze H J 1985 *Eur J Cell Biol* **38** 87-93
- [34] Beekman N J, Schaaper W M, Turkstra J A and Melen R H 1999 *Vaccine* **17** 2043-50
- [35] Gharavi A E, Pierangeli S S, Colden-Stanfield M, Liu X W, Espinola R G and Harris E N 1999 *J Immunol* **163** 2922-7
- [36] Bittle J L, Houghten R A, Alexander H, Shinnick T M, Sutcliffe J G, Lerner R A, Rowlands D J and Brown F 1982 *Nature* **298** 30-3
- [37] Strohmaier K, Franze R and Adam K H 1982 *J Gen Virol* **59** 295-306

